

# **Synthesis and Sequestering Properties of Enterochelin Analogues**

A dissertation submitted to The University of Manchester for the degree of Master of  
Chemistry by Research in the Faculty of Science and Engineering

**2019**

**Mohammad Khan**

**School of Chemistry**

## List of contents

1. Introduction.....	8
1.1 Synthesis and use for siderophores.....	9
1.2 Enterochelin.....	20
1.3 Biosynthesis of enterochelin.....	20
1.4 Chemical synthesis of enterochelin.....	22
1.5 Enterochelin analogue.....	24
2. Results and discussion.....	25
2.1 Aims and objectives.....	25
2.2 Synthesis of tert-butyl (2,3-dimethoxyphenyl) carbamate.....	27
2.3 Synthesis of 2,3 dimethoxyaniline hydrochloride.....	29
2.4 Synthesis of 2,3-dimethoxybenzenesulfonyl chloride.....	31
2.5 Synthesis of Methyl trityl-L-serinate.....	35
2.6 Synthesis of 2,2-dibutyl-1,3,2-dioxastannolane.....	37
2.7 Synthesis of (3S,7S,11S)-3,7,11-tris(tritylamino)-1,5,9-trioxacyclododecane-2,6,10-trione.....	39
3. Conclusion.....	41
4. Future work.....	42
5. Experimental.....	42
5.1 General experimental procedure.....	42
5.2 Synthesis of tert-butyl (2,3-dimethoxyphenyl) carbamate.....	43
5.3 Synthesis of 2,3 dimethoxyaniline hydrochloride.....	43
5.4 Synthesis of 2,3-dimethoxybenzenesulfonyl chloride.....	44
5.5 Synthesis of Methyl trityl-L-serinate.....	45
5.6 Synthesis of 2,2-dibutyl-1,3,2-dioxastannolane.....	46
5.7 Synthesis of (3S,7S,11S)-3,7,11-tris(tritylamino)-1,5,9-trioxacyclododecane-2,6,10-trione.....	47
6. References .....	48
7. Appendix .....	50
7.1 Infra-red spectroscopic data.....	50
7.2 Mass spectroscopy data.....	54

## List of figures

Figure 1 Structure of Rhodotorulic acid, enterochelin, foroxymithine and rhizoferrin .....	9
Figure 2 Oxinobactin and enterochelin .....	10
Figure 3 Synthesis of sideromycin, a mixed ligand siderophore-daptomycin conjugate.....	13
Figure 4 Chemical structure of erythrochelin .....	14
Figure 5 The biosynthesis of enterochelin on NRPS modules. ....	21
Figure 6 Enterochelin 2 and analogue of enterochelin 52.....	26
Figure 7 a) <sup>13</sup> C NMR and b) <sup>1</sup> H NMR of tert-butyl (2,3-dimethoxyphenyl) carbamate in chloroform- <i>d</i> .....	28
Figure 8 a) <sup>13</sup> C NMR and b) <sup>1</sup> H NMR of 2,3-dimethoxyaniline hydrochloride in methanol- <i>d</i> <sub>4</sub> .....	31
Figure 9 Diazonium intermediate.....	32
Figure 10 a) <sup>13</sup> C NMR and b) <sup>1</sup> H NMR of 2,3-dimethoxybenzenesulfonyl chloride in Chloroform- <i>d</i> .....	33
Figure 11 a) <sup>13</sup> C NMR and b) <sup>1</sup> H NMR of 1-chloro-2,3-dimethoxybenzene in Chloroform- <i>d</i> .....	34
Figure 12 a) <sup>13</sup> C NMR and b) <sup>1</sup> H NMR of Methyl trityl-L-serinate in Chloroform- <i>d</i> .....	36
Figure 13 a) <sup>13</sup> C NMR and b) <sup>1</sup> H NMR of Synthesis of 2,2-dibutyl-1,3,2-dioxastannolane in Chloroform- <i>d</i> .....	38
Figure 14 a) <sup>13</sup> C NMR and b) <sup>1</sup> H NMR of (3 <i>S</i> ,7 <i>S</i> ,11 <i>S</i> )-3,7,11-tris(tritylamino)-1,5,9-trioxacyclododecane-2,6,10-trione in Chloroform- <i>d</i> .....	40

## List of schemes

Scheme 1 Synthesis of the trilactone scaffold.....	11
Scheme 2 Protection and activation of 8-hydroxyquinolinecarboxylic acid.....	11
Scheme 3 Coupling step.....	12
Scheme 4 Synthesis of key building block of erythrochelin 2,5-DKP.....	15
Scheme 5 Synthesis of erythrochelin.....	16
Scheme 6 Synthesis of key intermediate.....	17
Scheme 7 Synthesis of chelator.....	18
Scheme 8 Synthesis of catecholamide compounds.....	19
Scheme 9 The Shanzer and Libman synthesis of enterochelin.....	23
Scheme 10 Synthesis of enterochelin by the direct cyclisation of Methyl trityl-L-serinate.....	24
Scheme 11 Full pathway for synthesis of enterochelin analogue.....	26
Scheme 12 Full pathway for synthesis of enterochelin analogue.....	27
Scheme 13 Synthesis of tert-butyl (2,3-dimethoxyphenyl) carbamate.....	27
Scheme 14 Synthesis of 2,3-dimethoxyaniline hydrochloride.....	29
Scheme 15 Synthesis of 2,3-dimethoxybenzenesulfonyl chloride.....	31
Scheme 16 Synthesis of Methyl trityl-L-serinate.....	35
Scheme 17 Synthesis of 2,2-dibutyl-1,3,2-dioxastannolane.....	37
Scheme 18 Synthesis of (3S,7S,11S)-3,7,11-tris(tritylamino)-1,5,9-trioxacyclododecane-2,6,10-trione.....	39

## Abstract

Acquisition of iron by siderophores is critical for the survival of many microbes. Enterochelin is a catechol siderophore that has a trilactonate macrocyclic core derived from serine that is connected to three 2, 3-dihydroxybenzoyl moieties all of which participate in the coordination of an iron atom in a hexadentate fashion. The work described in this thesis is concerned with the development of a viable synthetic pathway to a sulfonamide enterochelin analogue. Starting with L-Serine methyl ester hydrochloride and with the use of 2,2-dibutyl-1,3,2-dioxastannolane a synthetic pathway has been optimised for the synthesis of 3S,7S,11S)-3,7,11-tris(tritylamino)-1,5,9-trioxacyclododecane-2,6,10-trione enabling routine preparation on a multi-gram scale. Improvements have been made to the synthetic pathway towards the synthesis of 2,3-dimethoxybenzenesulfonyl chloride including a one-step conversion of tert-butyl (2,3-dimethoxyphenyl) carbamate to 2,3-dimethoxyaniline hydrochloride using HCl in dioxane.

## **Declaration**

No portion of the work referred to in the dissertation has been submitted in support of an application for another degree or qualification of this or any other university or other institute of learning.

## **Copyright statement**

The author of this dissertation (including any appendices and/or schedules to this dissertation) owns certain copyright or related rights in it (the “Copyright”) and he has given The University of Manchester certain rights to use such Copyright, including for administrative purposes.

Copies of this dissertation, either in full or in extracts and whether in hard or electronic copy, may be made **only** in accordance with the Copyright, Designs and Patents Act 1988 (as amended) and regulations issued under it or, where appropriate, in accordance with licensing agreements which the University has from time to time. This page must form part of any such copies made.

The ownership of certain Copyright, patents, designs, trademarks and other intellectual property (the “Intellectual Property”) and any reproductions of copyright works in the dissertation, for example graphs and tables (“Reproductions”), which may be described in this dissertation, may not be owned by the author and may be owned by third parties. Such Intellectual Property and Reproductions cannot and must not be made available for use without the prior written permission of the owner(s) of the relevant Intellectual Property and/or Reproductions.

Further information on the conditions under which disclosure, publication and commercialisation of this dissertation, the Copyright and any Intellectual Property and/or Reproductions described in it may take place is available in the University IP Policy, in any relevant Dissertation restriction declarations deposited in the University Library, The University Library’s regulations and in The University’s policy on Presentation of Dissertations.

## **Acknowledgement**

I would like to thank Dr Peter Quayle for his advice, guidance and support throughout the entirety of this programme of study.

I would also like to express my gratitude towards the members of the Quayle group for all their help and encouragement during my time with them.

Special thanks to my family for all their support and understanding.

## 1. Introduction.

In the natural world iron plays a fundamental role in the biological processes that occur in living organisms. Iron is able to coordinate and activate oxygen, processes which are inextricably linked to its ability to exist in a range of oxidation states and co-ordination geometries which are ideal for the transfer of electrons and reactions which are key to metabolic reactions. Paradoxically iron is not readily available for use in biological processes owing to the low solubility of iron(III) in water, even though iron is one of the most abundant elements found in the earth's crust. So to overcome this hurdle microorganisms, fungi and plants have evolved strategies to absorb iron from the environment.<sup>1</sup> One such mechanism used is to employ siderophores for the uptake of iron(III) even in environments with very low iron concentrations.<sup>2</sup>

Siderophores are organic compounds with a high affinity for iron(III), which chelate readily to form highly stable chelate complexes. Their high  $\text{Fe}^{3+}$  affinity means acquisition of iron via sequestration from sources that would normally be unavailable is possible.<sup>3</sup>

Being diverse in both structure and functional groups associated with the ligands that chelates to iron(III), siderophores can be categorized by the chemical moieties involved in iron binding;<sup>4</sup> these are catecholates, hydroxamates and carboxylates.<sup>1</sup> Examples of these can be seen in Figure 1. There are a number of siderophores classed as mixed-ligand siderophores that contain two or more types of ligands such as amyachelin and rhodochelin with the latter having a hydroxamate-aminocarboxylate binding motif while the former has a catecholate-hydroxamate mixed ligand structure.<sup>5</sup>



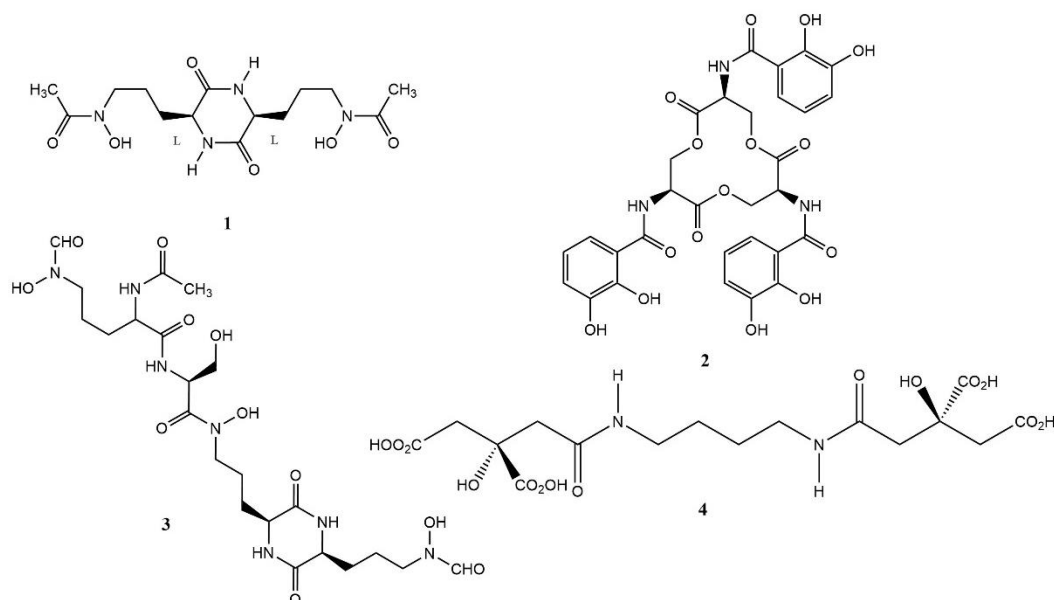


**Figure 1.** Structure of rhodotorulic acid **1**, enterochelin **2**, foroxymithine **3** and rhizoferrin **4**.

### 1.1 Synthesis and uses for siderophores

In recent studies, synthesis of novel siderophores have been reported for a variety of pharmaceutical applications.

An example of these new siderophores is detailed in a study done by du Moulinet d'Hardemare et al<sup>6</sup>. In it they describe the synthesis of oxinobactin **5** a siderophore analogue to enterochelin **2** but possessing 8-hydroxyquinoline instead of catechol complexing ligands (figure 2).

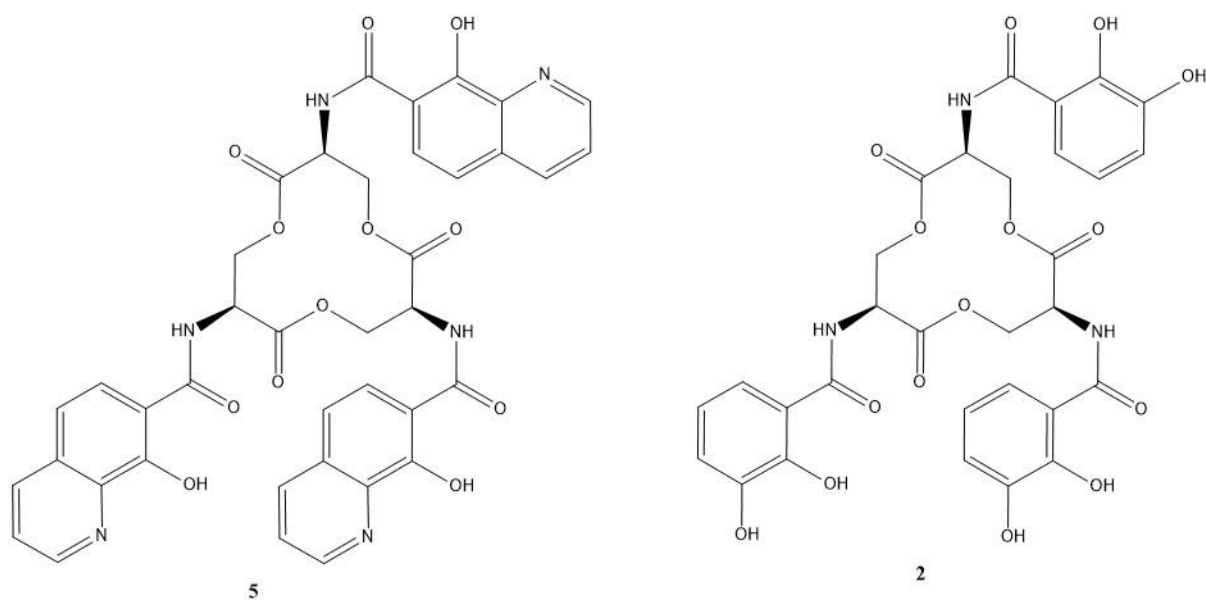
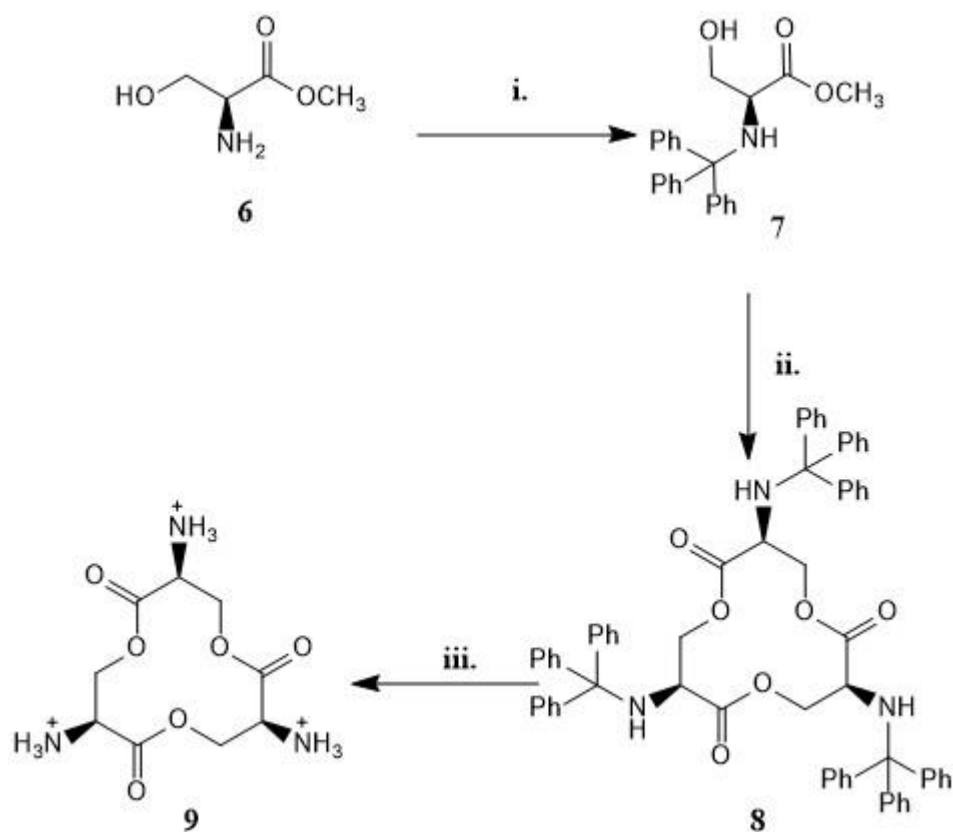
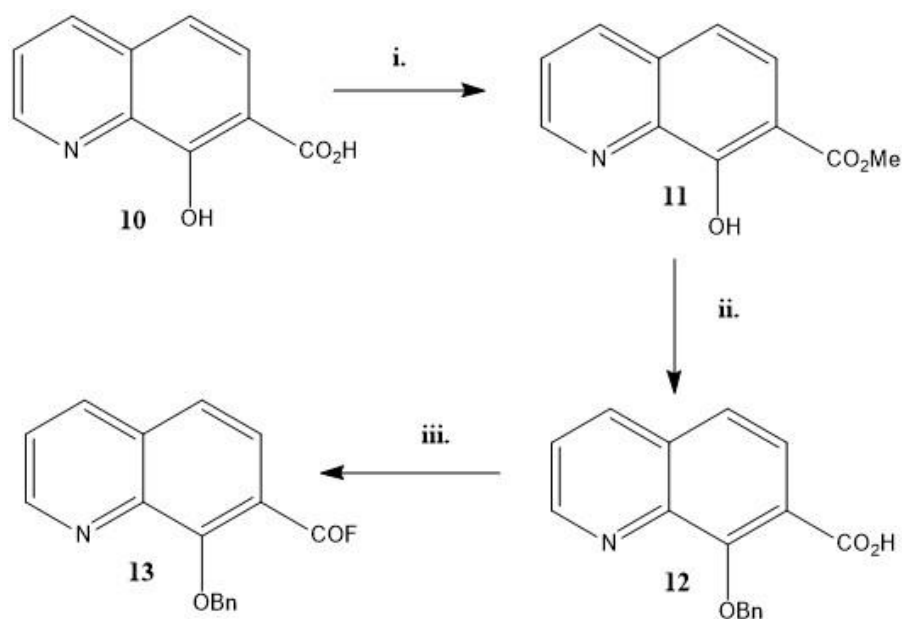


**Figure 2.** Oxinobactin **5** (with 8-hydroxyquinoline subunits) and enterochelin **2** (with catechol chelating subunits).

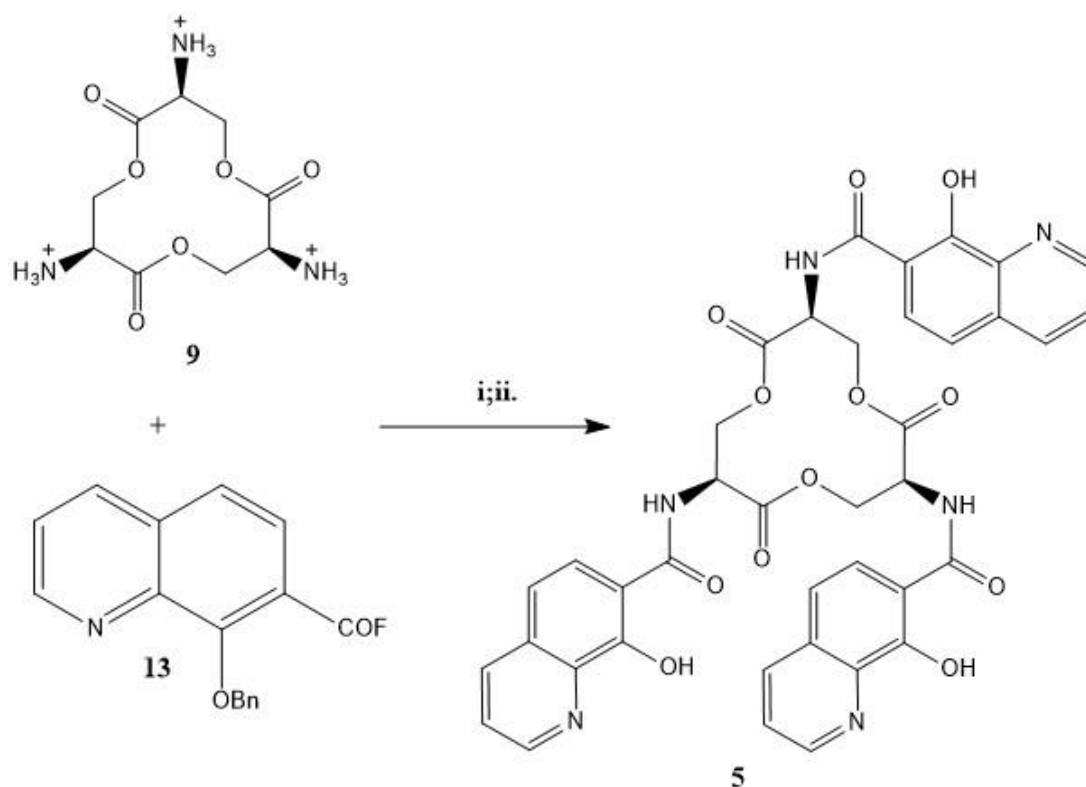
The synthesis of the siderophore was achieved by firstly making the trilactonate ring backbone **8** derived from L-serine **6**. The ring was then activated by removal of the trityl groups on the ring under acidic conditions to afford the salt **9** (scheme 1). The next step was protection of the phenol group of 8-hydroxyquinoline carboxylic acid (scheme 2). Finally, **9** and acid flouride **13** were coupled to give oxinobactin **5** in a 16% yield after deprotection (scheme 3).



**Scheme 1.** Synthesis of the trilactone scaffold **4**.<sup>6</sup> Reagents and conditions: (i) TrtCl, Et<sub>3</sub>N, CH<sub>2</sub>Cl<sub>2</sub>, 79%; (ii) 2,2-dibutyl-1,3,2-dioxastannolane, toluene, reflux, 75%; (iii) HCl, EtOH, rt, 95%



**Scheme 2.** Protection and activation of 8-hydroxyquinolinecarboxylic acid.<sup>6</sup> Reagents and conditions: (i) BF<sub>3</sub>, MeOH, reflux, 97%; (ii) BnCl, K<sub>2</sub>CO<sub>3</sub>, KI, EtOH, reflux, 95%; then NaOH, MeOH, reflux, then pH 7, 82%; (iii) C<sub>3</sub>F<sub>3</sub>N<sub>3</sub>, DIPEA, CH<sub>2</sub>Cl<sub>2</sub>, 0 °C, 75%



**Scheme 3.** Coupling step.<sup>6</sup> Reagents and conditions: (i) DIPEA, CH<sub>2</sub>Cl<sub>2</sub>, 0 °C, 66%; (ii) H<sub>2</sub>, Pd/C, EtOH, 16%.

Siderophore **5** was tested against enterochelin for iron(III) complexing ability. It was found that at neutral pH **5** was as strong a chelator of iron(III) as **2** and actually was more efficient at lower pH than **2**. Owing to the results obtained by du Moulinet d'Hardemare et al. they gave possible applications for oxinobactin such as chelation therapy especially in neurodegenerative diseases and as a possible receptor for pathogenic microorganisms.

Ghosh et al.<sup>7</sup> reported the synthesis of a siderophore-antibiotic conjugate sideromycin **17**. This was done by attaching a synthetic siderophore **14** to daptomycin **16** using a glutarate linker (figure 3). The aim was to test the effectiveness of **17** as a potential trojan horse delivery system of antibiotic **16** in bacterial cells.

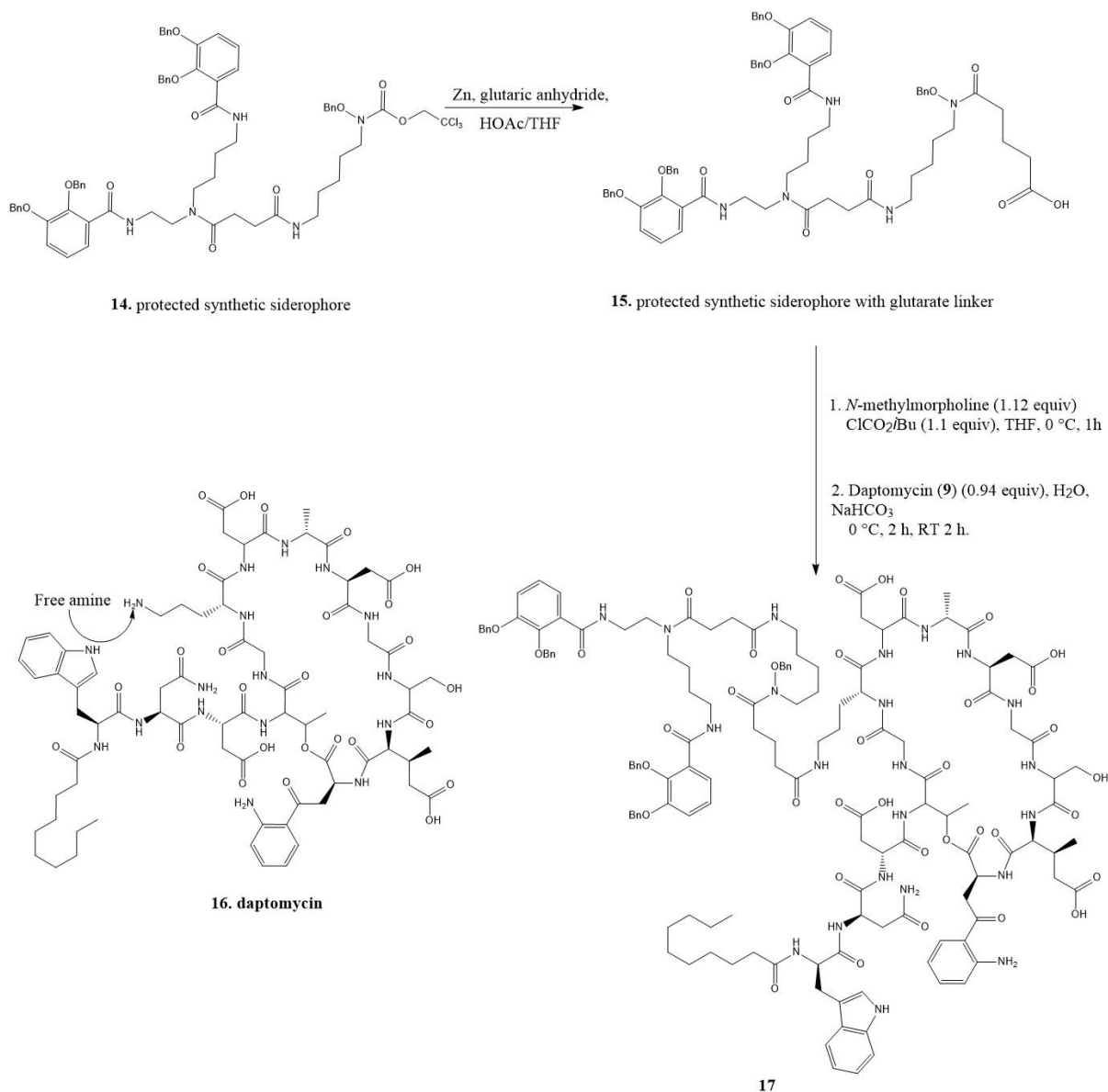


**Figure 3.** Synthesis of sideromycin **17**, a mixed ligand siderophore-daptomycin conjugate.<sup>7</sup>

Results obtained during the study indicated that conjugation of siderophores to antibiotics such as daptomycin that are much larger than the siderophore (iron chelator) itself facilitates active uptake that circumvents the normal permeability problems in Gram- negative bacteria. Structure of the siderophore and choice of linker were important in the success of the conjugate. Iron binding stoichiometry and structural aspects of the iron coordination sphere also required consideration with respect to the iron binding motifs used.

In work carried out by Nakao et al.<sup>8</sup> a hydroxamate-type siderophore erythrochelin **18** produced by a pathogenic bacterial cell was synthesised. This was the first reported synthesis of **18**.

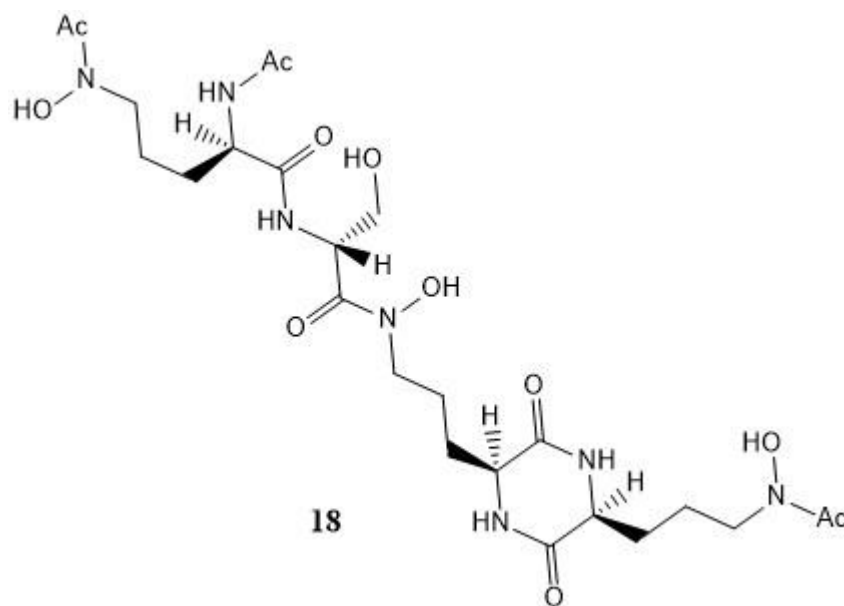
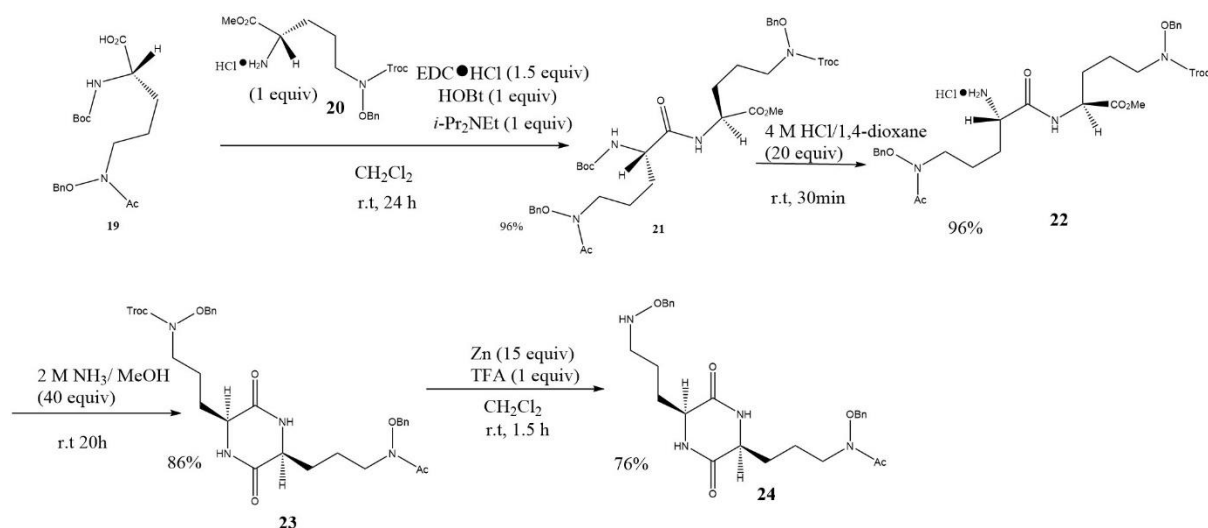


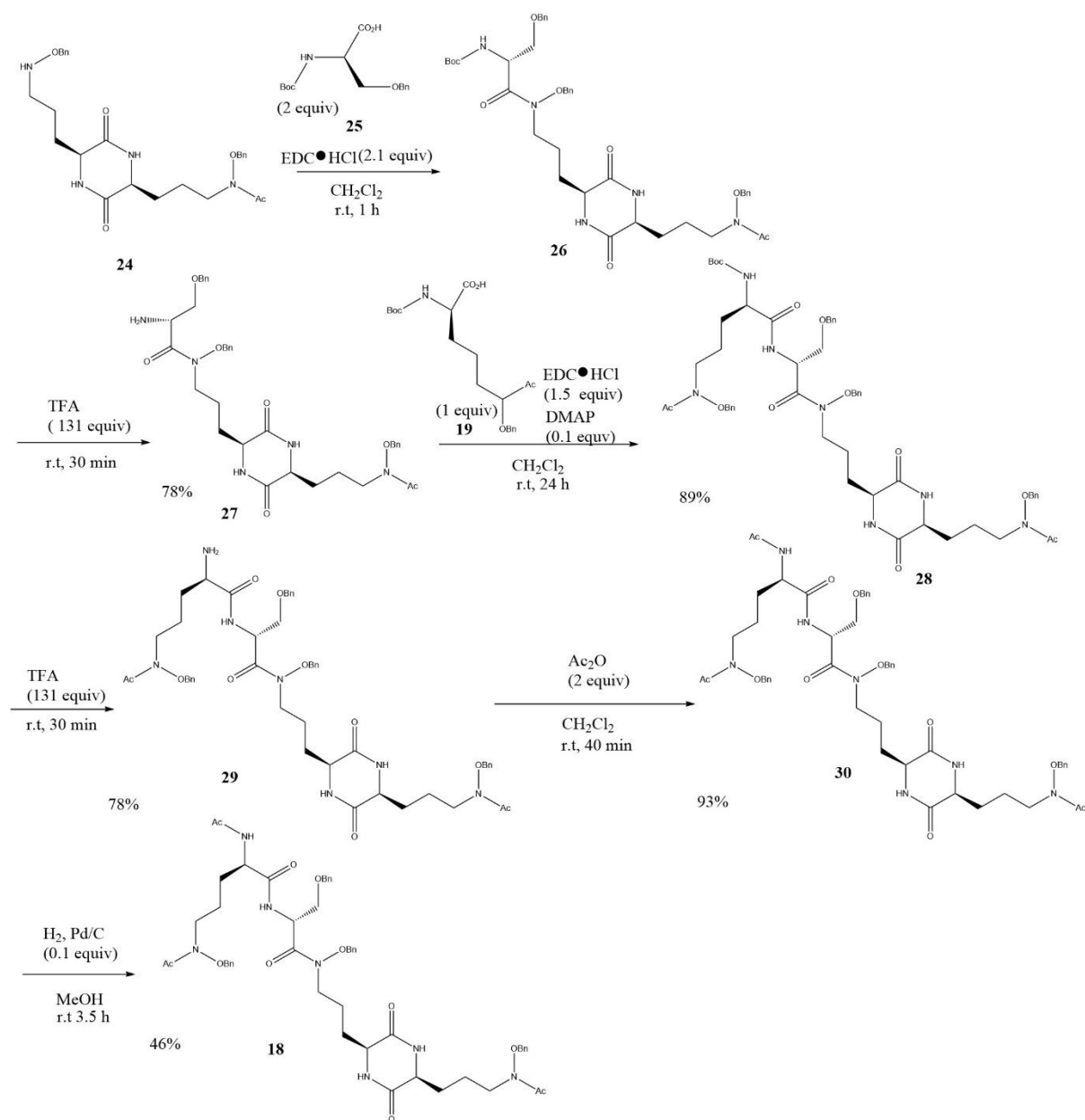
**Figure 4.** chemical structure of erythrochelin

Firstly protected amino acids **19** and **20** underwent a condensation reaction using 1-ethyl-3-(3-dimethylaminopropyl)carbodiimide hydrochloride (EDC·HCl) as a coupling reagent in the presence of 1-hydroxybenzotriazole (HOBt) and N,N-diisopropylethylamine (DIPEA). Peptide **21** was obtained in a 96% yield. Then deprotection of **21** with an excess amount of 4 M HCl in 1,4-dioxane afforded the dipeptide methyl ester hydrochloride salt **22** in 96% yield. Intramolecular cyclisation of **22** on treatment with ammonia solution (2 M in MeOH) afforded **23** in 86% yield. Reductive removal of the 2,2,2-trichloroethoxycarbonyl (Troc) protecting group of **23** with an excess of zinc powder in the presence of trifluoroacetic acid (TFA) gave the key building block **24** in 76% yield (scheme 4).



**Scheme 4.** Synthesis of key building block of erythrochelin 2,5-DKP **24**.<sup>8</sup>

For the next step of the synthesis the building block **24** was coupled via condensation reaction to **25** using EDC·HCl to provide **26**. Subsequent deprotection of **26** using an excess of TFA afforded **27** in 74% yield. Amine **27** was then coupled with an equivalence of **19** to form **28** in 89% yield. Deprotection of **28** meant that **29** (78% yield) was obtained and then acetylation using acetic anhydride gave **30** in 96% yield. The final step was catalytic hydrogenolysis under hydrogen with palladium on carbon which gave erythrochelin **18** in 46% yield after recrystallisation (scheme 5).

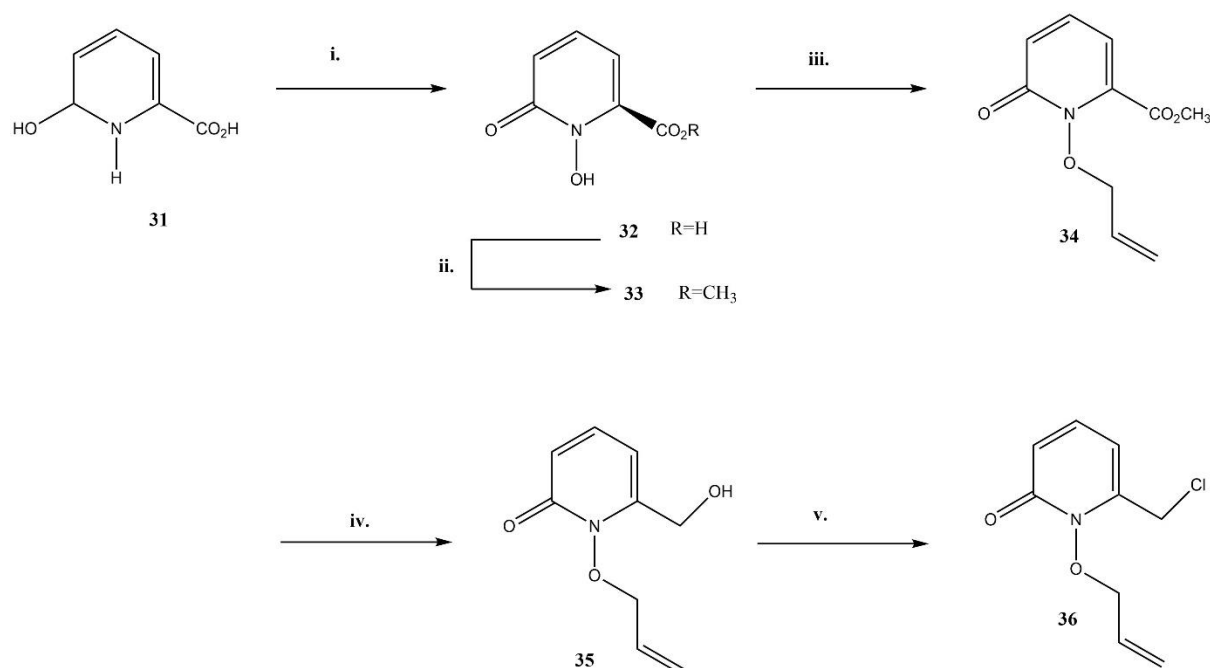


**Scheme 5.** Synthesis of erythrochelin **18**.<sup>8</sup>

Workman et al.<sup>9</sup> detailed the synthesis of novel chelators based on 1-hydroxy-2(1H)-pyridinone coordinating groups decorating a triazamacrocyclic backbone. These were powerful iron(III) chelators capable of competing with bacterial siderophores. They found that when tested with bacterial cells ligands had a demonstratable biostatic effect upon the growth of a range of the microbes. The rate of growth was significantly reduced with increasing concentrations of chelators.

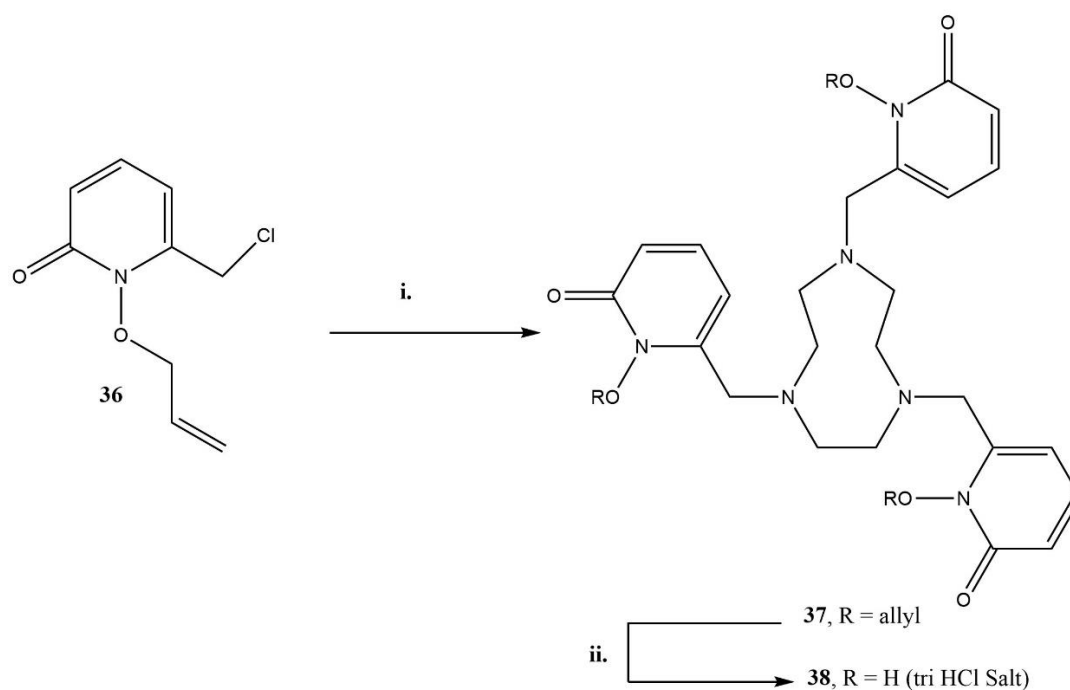


For one of the chelators synthesised by the group a key allyl protected 6-hydroxymethyl intermediate **34** was synthesised in a five-step series from commercially available starting material **31**. The hydroxymethyl derivative **35** was then converted to the key intermediate **36** using thionyl chloride (Scheme 6).



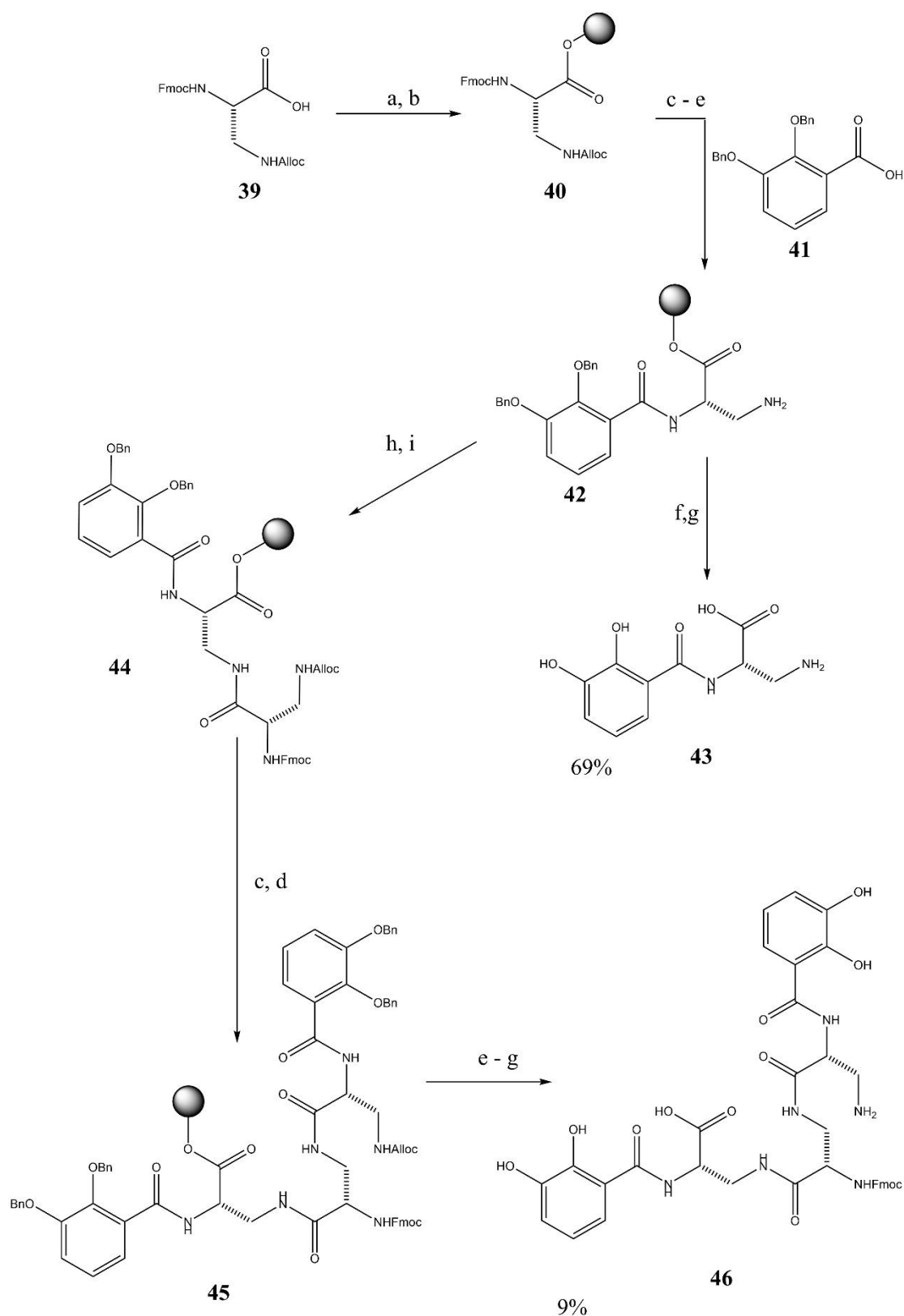
**Scheme 6.** Synthesis of key intermediate **36**.<sup>9</sup> reagents and conditions: (i)  $\text{CH}_3\text{CO}_3\text{H}$ ,  $\text{AcOH}$ ,  $80^\circ\text{C}$ ; 77% (ii)  $\text{MeOH}$ ,  $\text{SOCl}_2$ , reflux; 96% (iii)  $\text{CH}_2\text{CHCH}_2\text{Br}$ ,  $\text{K}_2\text{CO}_3$ , acetonitrile, reflux; 94% (iv)  $\text{NaBH}_4$ ,  $\text{MeOH}$ ,  $\text{THF}$ , reflux; 65% (v)  $\text{SOCl}_2$ ,  $\text{CH}_2\text{Cl}_2$ , reflux; 92%.

For the next step a reaction, three equivalents of **36** with 1,4,7-triazacyclononane in the presence of potassium carbonate produced the allyl protected macrocyclic product **37** in a yield of 93%. The removal of the allyl protecting group was performed using boron trichloride, without cleavage of the newly formed carbon-nitrogen bond, to give chelator **38** (scheme 7).



**Scheme 7.** Synthesis of chelator **38**. Reagents and conditions: (i) TACN, K<sub>2</sub>CO<sub>3</sub>, CH<sub>3</sub>CN, reflux; 93% (ii) BCl<sub>3</sub>, CH<sub>2</sub>Cl<sub>2</sub>; 87%.<sup>9</sup>

Zamora et al<sup>10</sup> have developed a solid-phase synthesis of catecholamide compounds modelled on enterochelin fragments (scheme 8). Compounds **43** and **46** were prepared by applying a solid-phase synthesis (SPS) approach, which offers practical advantages over solution-phase synthesis for this class of compounds such as easier isolation of products and higher yields.



**Scheme 8.** Synthesis of catecholamide compounds **43** and **44**.<sup>10</sup> (a) 2-Chlorotrityl chloride resin, DIPEA, CH<sub>2</sub>Cl<sub>2</sub>, rt, 1 h; (b) CH<sub>2</sub>Cl<sub>2</sub>, DIPEA, MeOH, rt, 30 min; (c) 4-Methyl-piperidine 20% in DMF, 20 min, rt; (d) HBTU, 5, DIPEA, DMF, rt, 45 min; (e) Pd(PPh<sub>3</sub>)<sub>4</sub>, PhSiH<sub>3</sub>, THF, rt, 20 min; (f) CH<sub>2</sub>Cl<sub>2</sub>, TIPS, TFA; (g) Pd(OH)<sub>2</sub>H<sub>2</sub>, MeOH, rt, 30 min; (h) HBTU, Alloc-Dap(Fmoc)-OH (**3**), DIPEA, DMF, 45 min; (i) Alloc-Cl, DIPEA, CH<sub>2</sub>Cl<sub>2</sub>, rt, 1 h.

This synthetic route starts from **39**, which was immobilized on 2-chlorotrityl polystyrene supported resin giving **40**. Fmoc deprotection of **40** with 4-methylpiperidine in DMF, followed by reaction **41** afforded the fully protected **42**. Then *N*-Alloc group removal was carried out with the palladium catalyst (Pd(PPh<sub>3</sub>)<sub>4</sub>) and phenylsilane (PhSiH<sub>3</sub>), giving **41**. After cleavage from the resin and a Pd/C-catalysed hydrogenolysis the final compound **43** was obtained. For the synthesis of biscatechol **46**, a second equivalent of **39** was attached using HBTU-mediated coupling, followed by carbamate reinstallation with allyl chloroformate (Alloc-Cl) to address partial deprotection, giving compound **44**. In the final immobilized step, **41** was conjugated to **44** after removal of the protecting group to yield compound **45**. Removal from the resin and subsequent hydrogenolysis afforded **46** in modest yields.

## 1.2 Enterochelin

Enterochelin **2** is a catecholate type of siderophore which is produced by bacteria such as *Escherichia coli*, *Salmonella typhimurium* and *Klebsiella pneumoniae*.<sup>11</sup> It has a trilactonate macrocyclic core derived from serine that is connected to three 2, 3-dihydroxybenzoyl moieties which participate in the coordination of an iron atom<sup>12</sup>. They bind in a hexadentate fashion and are integrated into a conformationally restrained scaffold that adopts an pseudooctahedral geometry around iron(III).<sup>13</sup> Enterochelin can bind to iron(III) very tightly with a stability constant of  $10^{52} \text{ M}^{-1}$  meaning it has one of the highest affinities of all siderophores<sup>14</sup>.

The isolation of enterochelin was reported in 1970 by two pairs of researchers who worked independently of each other; they were O'Brien and Gibson<sup>15</sup> and Pollack and Neilands<sup>16</sup>. The former pair isolated **2** from *E. coli* and the latter pair obtained it from *Salmonella typhimurium*.

## 1.3 Biosynthesis of enterochelin

The majority of siderophores are biosynthesised by nonribosomal peptide synthetases (NRPSs). These synthetases are essentially assembly lines of specialised domains that link amino acids via thioester intermediates.<sup>17</sup> The coordinated biosynthesis of NRPSs

(involved with siderophore synthesis) is activated by promoters which are sensitive to iron depletion.<sup>1</sup>

Enterochelin **2** uses dihydroxybenzoic acid and serine as building blocks (figure 4). The dihydroxybenzoic acid acts as an N-capping substrate for the NRPS and the assembly system forms ester links (instead of amide links) between the capped serine molecules.<sup>17</sup>

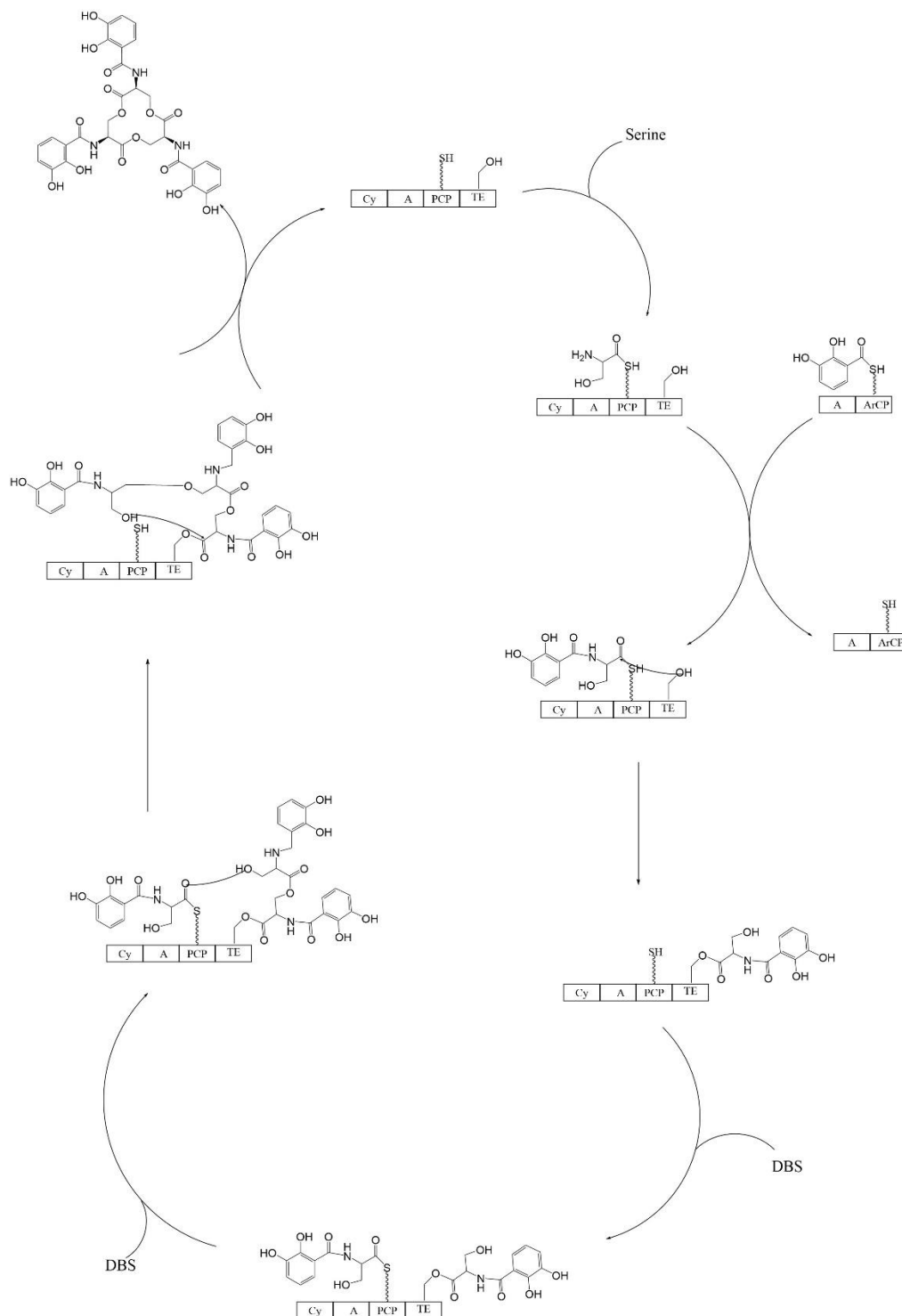
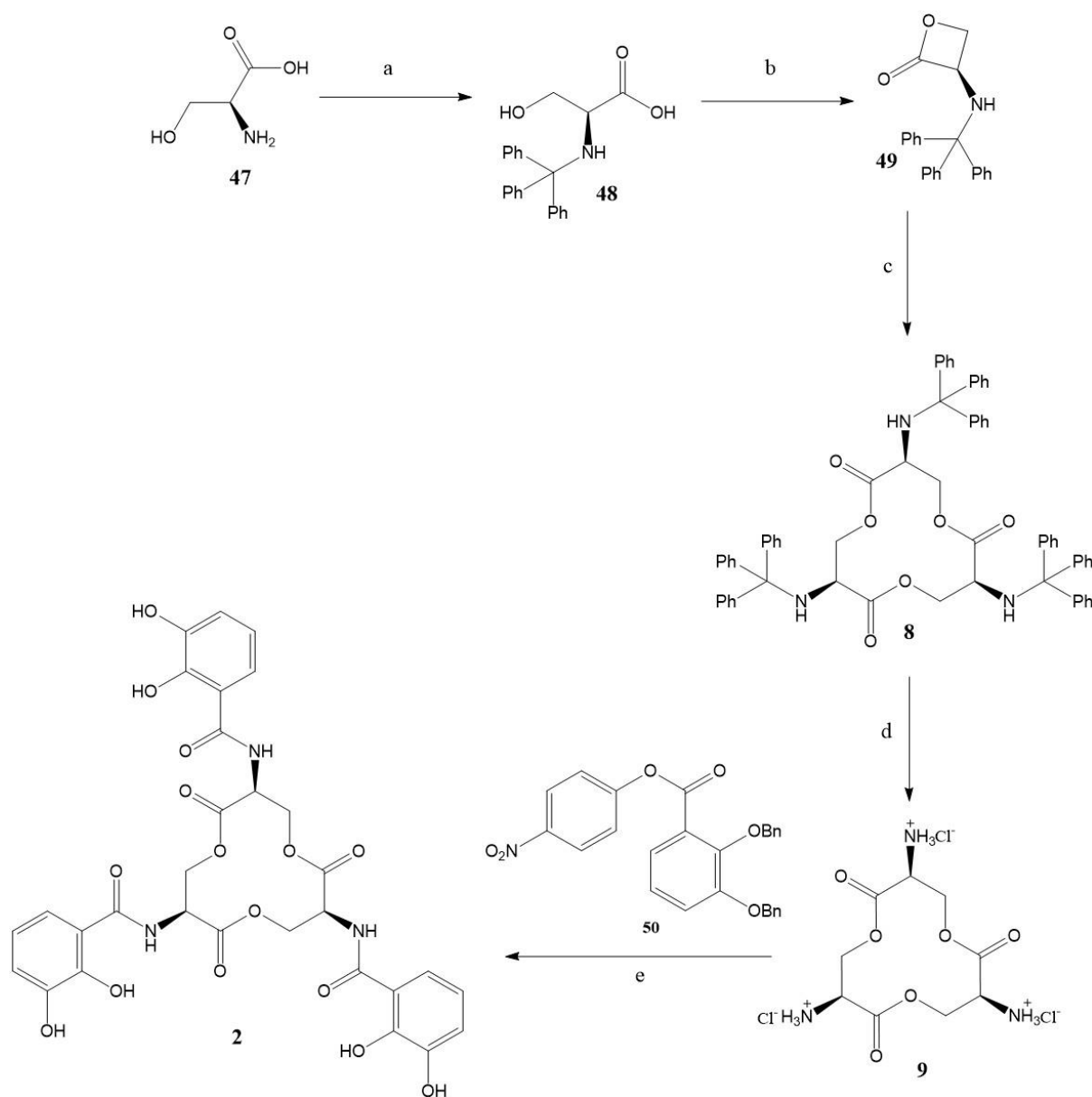


**Figure 5.** The biosynthesis of enterochelin **2** on NRPS modules.<sup>1</sup>

## 1.4 Chemical synthesis of enterochelin

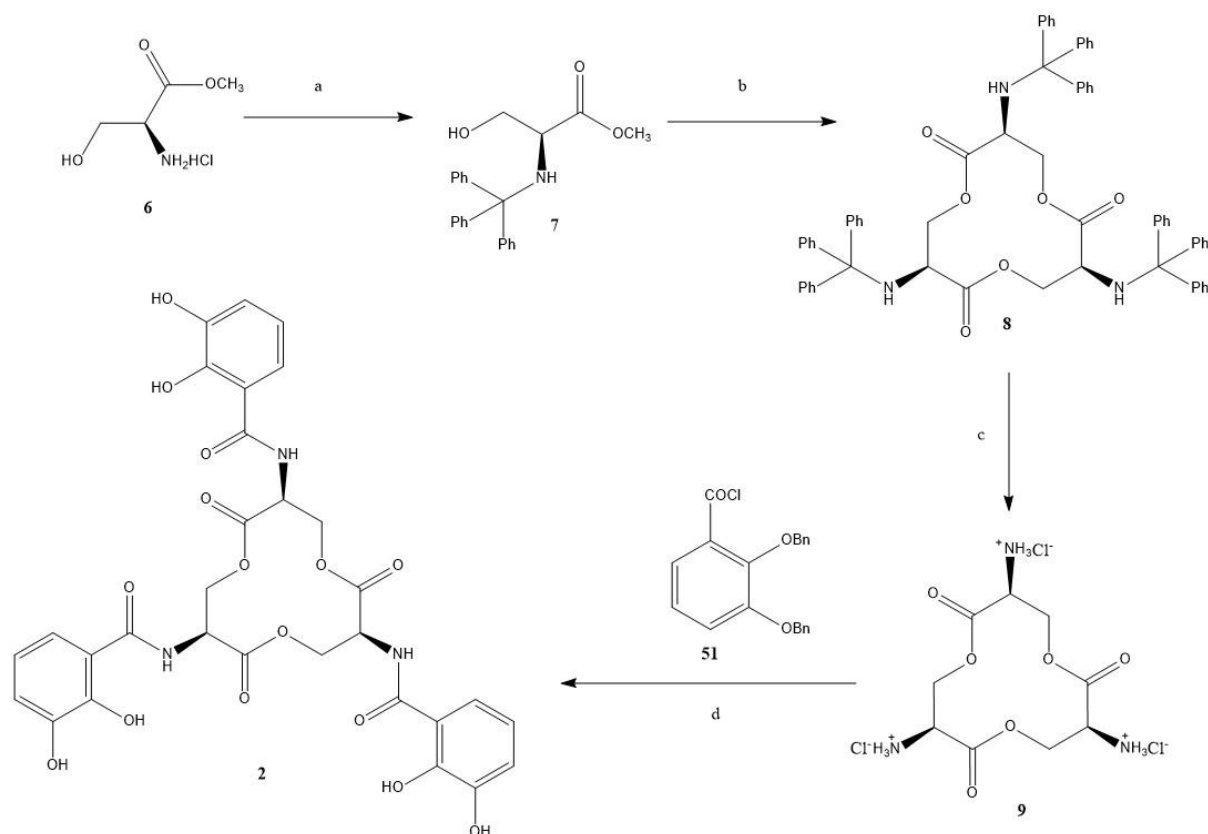
The first synthesis of enterochelin **2** was reported by Corey and Bhattacharya in 1977,<sup>18</sup> in an undisclosed yield. In the years that followed various other studies<sup>19,20</sup> (adopting the basic strategy of Corey and Bhattacharya's work) were conducted into the synthesis of enterochelin, - all of which resulted in low yields.

A different strategy to the synthesis of **2** was implemented by Shanzar and Libman<sup>21</sup> (scheme 9). Unlike the previously mentioned studies,<sup>18, 19</sup> which relied on the stepwise condensation of serine derivatives to a linear trimer and then subsequent cyclization of the trimer, Shanzar and Libman developed a method based on the use of cyclic tin-oxide compounds as templates in the self-condensation of  $\beta$ -lactones to the macrocyclic lactonate. It was reported the key trimerization step afforded trilactone **8** in 23% yield. From the X-ray studies carried out they found that of the three trityl groups on each side chain of **8** two were equatorial and one was in an axial orientation.<sup>22</sup>



**Scheme 9.** The Shanzer and Libman synthesis of enterochelin **2**.<sup>21</sup> Reagents and conditions: a) Et<sub>3</sub>N, TrCl, 48 h, 0 °C; b) dry DCM, 0 °C, DMAP, DIC, 2 days, r.t, 26%; c) 2,2-dibutyl-1,3,2-dioxastannolane, dry CHCl<sub>3</sub>, 2.2 h, reflux, 23%; d) 1M HCl, EtOH, 2 min; e) 1. Et<sub>3</sub>N, dry DCM; 2.H<sub>2</sub>, Pd/C, EtOH.

More recent studies have refined and developed this strategy, where the formation of **49** by using L-Serine methyl ester **6** in place of **47** as the starting material (scheme 10). This allowed direct cyclisation of methyl trityl-L-serinate **7** to trillactone **8**. Yields were much higher as a result (65-80% depending on solvent used)<sup>23,24</sup>. Trillactone **8** was transformed into salt **9** by reaction with HCl. The salt was converted into enterochelin **2**, in a 70% yield, by reaction with 2,3-dibenzyloxybenzoyl chloride **55** followed by hydrogenolysis of the benzyloxy protecting groups (OBn).<sup>25</sup>



**Scheme 10.** Synthesis of enterochelin **1** by the direct cyclization of **7**.<sup>23,24</sup> Reagents and conditions: a) Et<sub>3</sub>N, TrCl, 48 h, 0°C; b) 2,2-dibutyl-1,3,2-dioxastannolane, *m*-xylene, 96 h, reflux, c) ethanolic HCl, 2 h, r.t and d) 2,3-bis(benzyloxy)benzoyl chloride **55**, H<sub>2</sub>, Pd-C.

### 1.5 Enterochelin analogue

Research carried out by A. Bukhari from the Quayle group detailed the synthesis of a sulfonamide analogue **52** of enterochelin **2**.<sup>26</sup> The difference between the two was that **52** had sulfonamide linkage between the macrocycle backbone and catechol moieties instead of amides (figure 6).



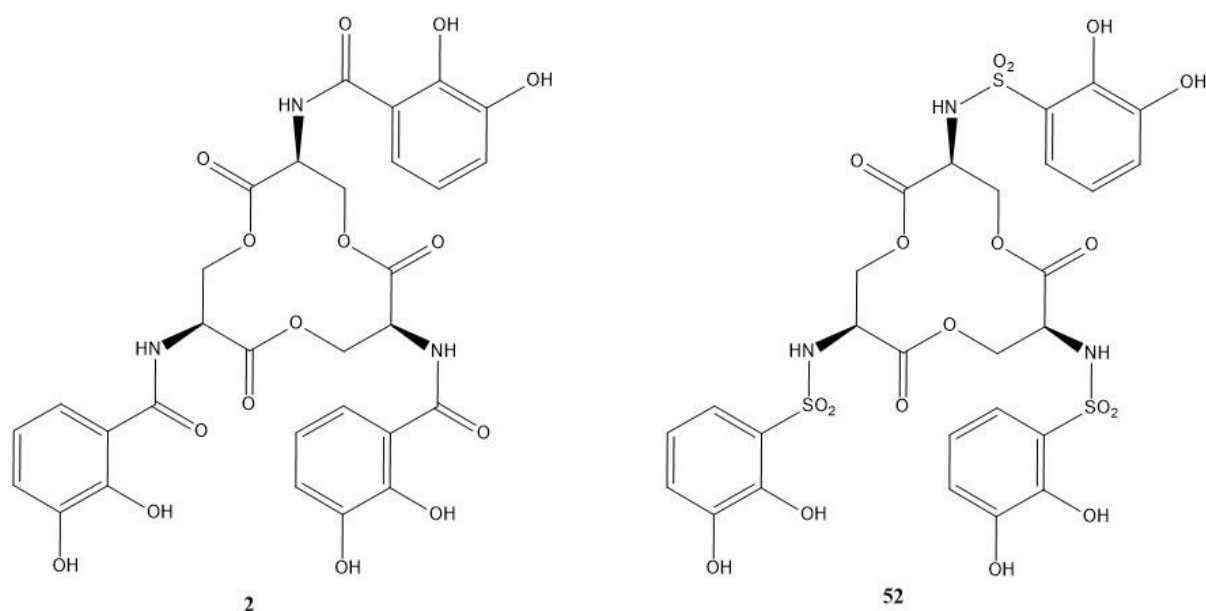


**Figure 6.** Enterochelin **2** and analogue of enterochelin **52**

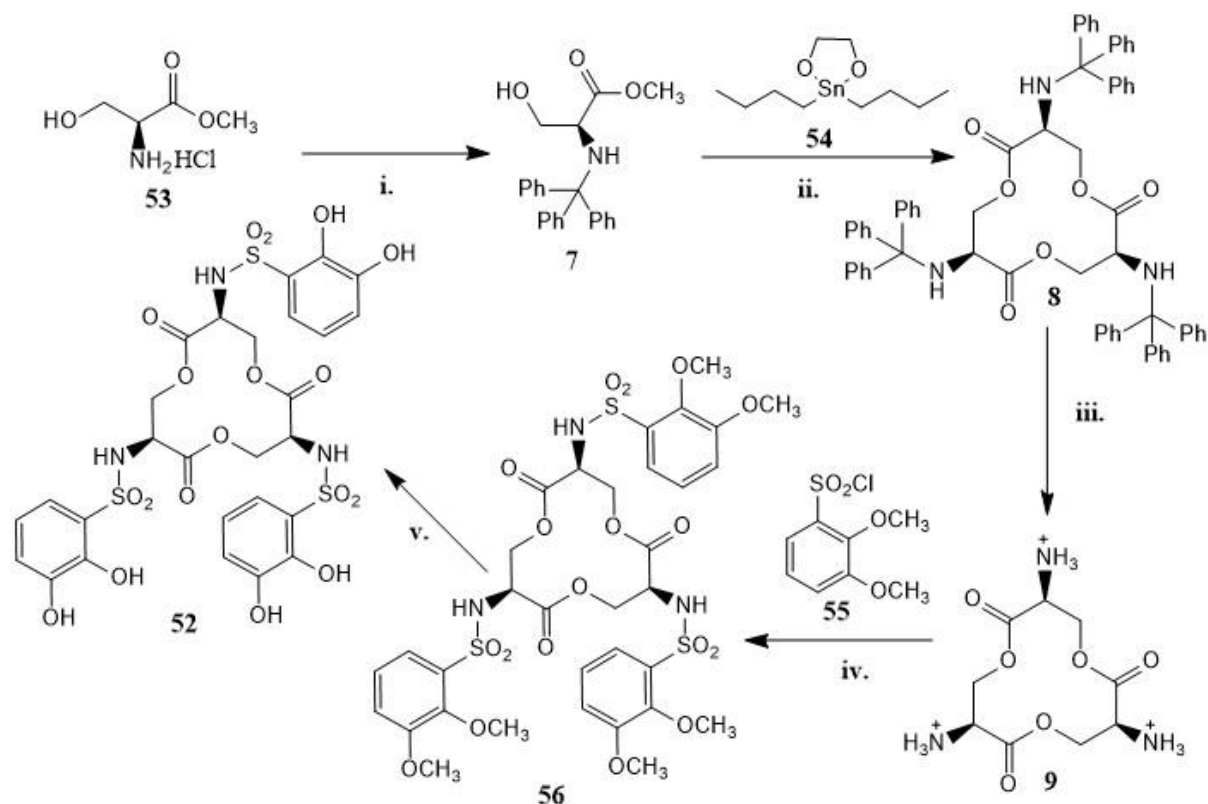
The synthesis pathway developed by Bukhari was not optimised and insufficient quantities of **52** had been prepared to be able to test its activity as a chelator of iron(III). In order to carry out these studies the synthesis of **52** on a gram scale would be required and it was the aim of this project to repeat Bukhari's synthesis of **52** so that each of the steps proceeded in a reproducible manner.

## 2.Results and discussion

### 2.1 Aims and objectives

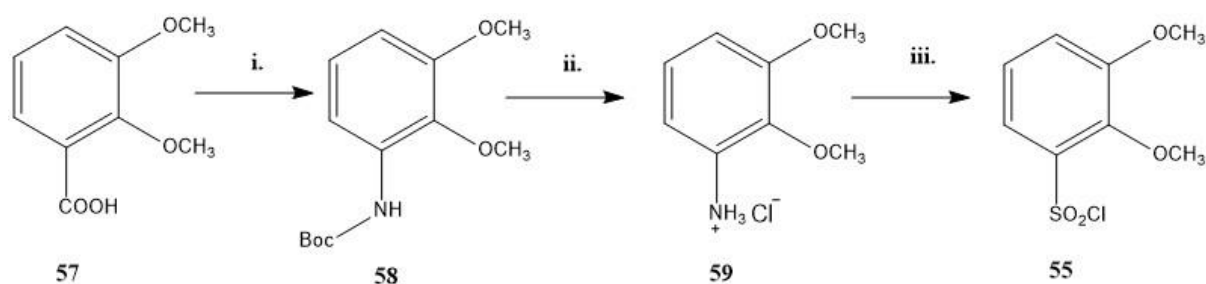
The main aims of this research project were to synthesise the sulfonamide analogue of enterochelin **52** by following a strategy of synthesis which had been set out by a former member of the Quayle group. Research into the synthesis of enterochelin analogues had been carried out by A.Bukari<sup>26</sup>, who had developed a potentially robust synthetic route. The synthetic route was to be followed and to be checked for its reproducibility of results. On successful synthesis of **52** there were further aims to look at the effectiveness of the ligand at sequestering iron (III). This would be done to test the suitability of the analogue as a potential conjugate for an effective 'trojan horse' antibiotic delivery system.<sup>27</sup>

A post functionalisation approach would be adopted in the synthesis of the sulfonamide analogue **52**. This meant that the trilactonate **8** backbone of the analogue would be synthesised and then after subsequent activation used to couple with sulfonyl chloride **55** to obtain the protected analogue **56**. Deprotection in the next stage would afford the desired enterochelin analogue **52** (scheme 11).



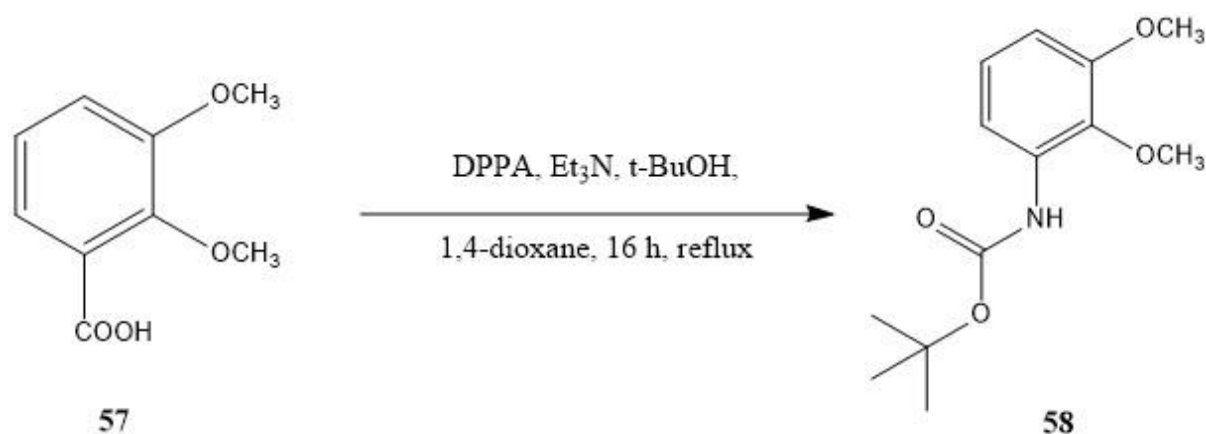
**Scheme 11.** Full pathway for synthesis of enterochelin analogue. Reagents and conditions: i) Et<sub>3</sub>N, TrCl, 48 h, 0°C; ii) m-xylene, 72 h, reflux, iii) ethanolic HCl, 2 h, r.t ; iv) Et<sub>3</sub>N, 0.5 h at 0°C, 1.5 h at r.t; v) BBr<sub>3</sub>, 2 h at -10°C, MeOH 30 min at -78°C, H<sub>2</sub>O.

The proposed synthesis of the sulfonyl chloride **55** was to be a three-step reaction sequence (scheme 12). Starting from commercially available 2,3-dimethoxybenzoic acid **57** as starting material Curtius-type rearrangement<sup>28</sup> promoted by diphenyl phosphoryl azide (DPPA) was to be employed in the synthesis of carbamate **58**. Selective deprotection of **58** to **59**, followed by diazotisation and sulfonation (Meerwein's procedure<sup>29</sup>) to the sulfonyl chloride **55** was to complete the sequence.



**Scheme 12.** Full pathway for synthesis of enterochelin analogue. Reagents and reaction condition: i) DPPA, Et<sub>3</sub>N, t-BuOH, 1,4-dioxane, 16 h, reflux; ii) KOH, EtOH, H<sub>2</sub>O, 115 °C then HCl/EtOH, 24 hrs and iii) 1. NaNO<sub>2</sub>, HCl, AcOH, CH<sub>3</sub>CN, 0.5 h, 0 °C; 2. SO<sub>2</sub>(g), CuCl<sub>2</sub>.2H<sub>2</sub>O, 0.5 h, 0 °C, 16 h, r.t.

## 2.2 Synthesis of tert-butyl (2,3-dimethoxyphenyl) carbamate (58)



**Scheme 13.** Synthesis of tert-butyl (2,3-dimethoxyphenyl) carbamate **58**.

Using the readily available dimethoxyphenyl carboxylic acid **57** the reaction was carried out. The triethylamine acted as a base and DPPA and t-BuOH were used to make the carbamate group via Curtius type rearrangement. The crude product obtained after reflux was purified via column chromatography using a 2:8 ethyl acetate: petroleum ether eluent which afforded **58** in a 60% yield. Though the yield obtained was moderate the ease of the procedure and purification allowed for successful scale up reactions that also gave 60% yields.

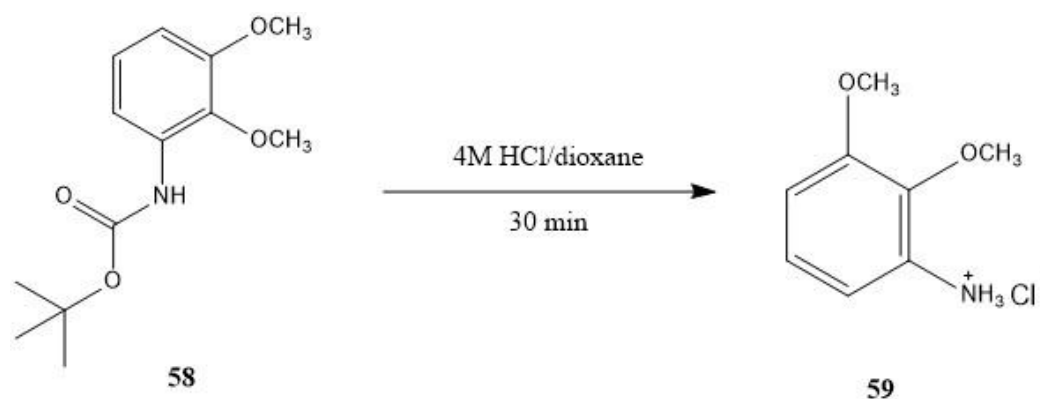
<sup>1</sup>H and <sup>13</sup>C NMR spectroscopy of the carbamate confirmed the presence of 7 distinct proton environments and 11 carbon environments. The proton NMR also revealed that the two methoxyphenyl groups are not equivalent in terms of proton environment. MS showed a peak

**Figure 7.** a)  $^{13}\text{C}$  NMR spectrum and b)  $^1\text{H}$  NMR spectrum of **58** in chloroform-*d*.



**Figure 7.** a)  $^{13}\text{C}$  NMR spectrum and b)  $^1\text{H}$  NMR spectrum of **58** in chloroform-*d*.

### 2.3 Synthesis of 2,3-dimethoxyaniline hydrochloride (**59**)



**Scheme 14.** Synthesis of 2,3-dimethoxyaniline hydrochloride

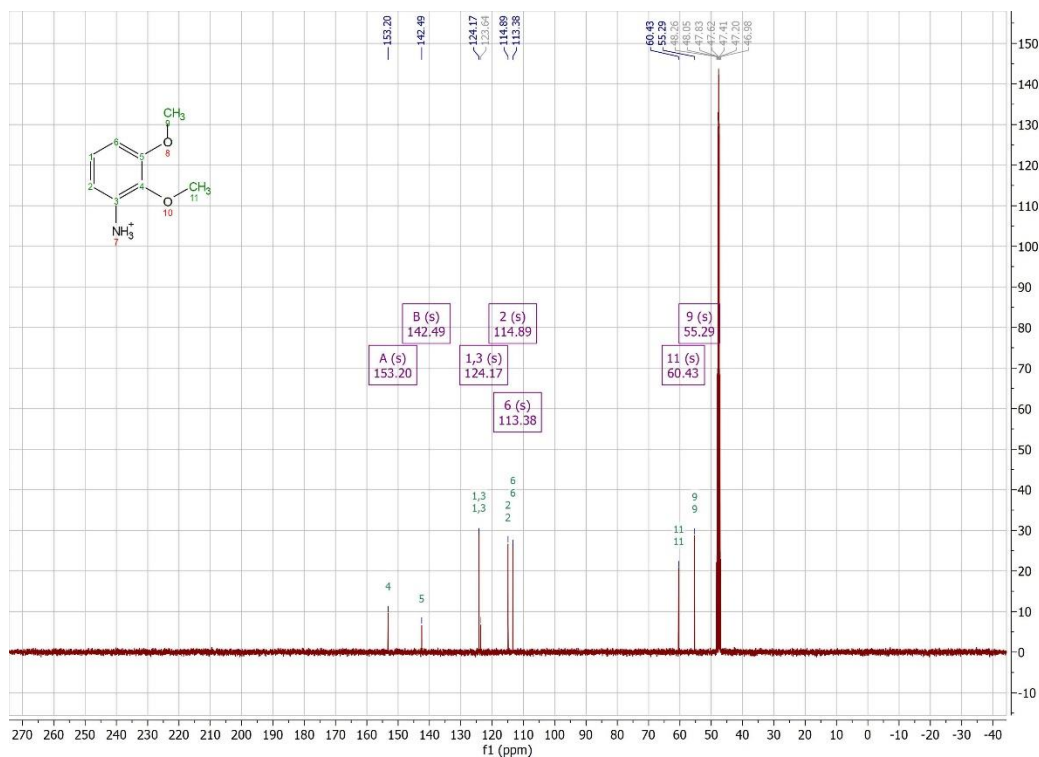
The original strategy for the formation of **59** was to use KOH as a base to remove the protecting Boc group from **58** to obtain the dimethoxyaniline after work-up. This would then be reacted with HCl to form the salt **59**. In practice however, multiple attempts (varied reaction temperature 90-120°C; stirring time changed to 12 hr and different purification method tried) yielded the starting material carbamate **58**. With the method not working an alternative method was devised.

An excess of 4M HCl in dioxane was mixed with **58**. The mixture was heated to reflux for 30 minutes with stirring, after filtration a yellow solid was obtained in 82% yield. This method provided a pathway straight from the carbamate to **59** with a high yield.

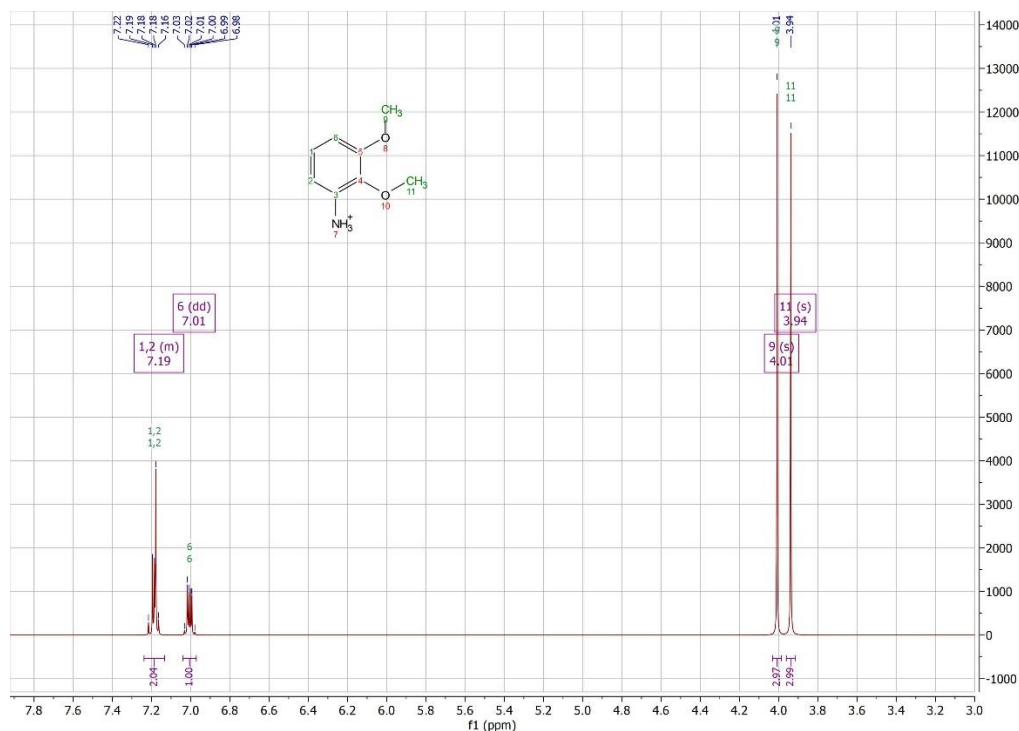
The  $^1\text{H}$  and  $^{13}\text{C}$  NMR spectra of the salt **59** in methanol- $d_4$  confirmed the presence of 4 distinct proton environments and 7 carbon environments. A melting point of 210-212 °C was observed which was considerably higher than what had been reported in the literature (177-178 °C).<sup>26</sup> The reason for this may be that a different synthesis pathway has been used leading to a different crystal form. Another possibility is that the synthesised compound **59** was in a purer form than obtained previously. When the HRMS required value for  $\text{C}_8\text{H}_{11}\text{NO}_2$  ( $m/z$  154.0863,  $\text{MH}^+$ ) was compared to the found value of  $m/z$  154.0858 it was seen there was very little difference in the values meaning the yellow solid obtained was indeed **59**. As the compound was crystalline a microanalysis of the elemental proportions was carried to further confirm the composition and purity of the yellow crystalline solid. The data obtained from the analysis

(C<sub>8</sub>H<sub>12</sub>NO<sub>2</sub> requires C 50.66, H 6.33, N 7.39, Cl 18.73%; found C 50.83, H 6.40, N 7.32, 18.59 %) further confirmed the fact that the target of the HCl salt **59** had been achieved.

The procedure which was employed to successfully make **59** was found to be scalable to larger quantities (40 mmol) without negatively effecting the yield. Due to it being a one step procedure with very minimal work-up it was a general improvement to the target HCl salt procedure used in the original literature<sup>26,28</sup>.



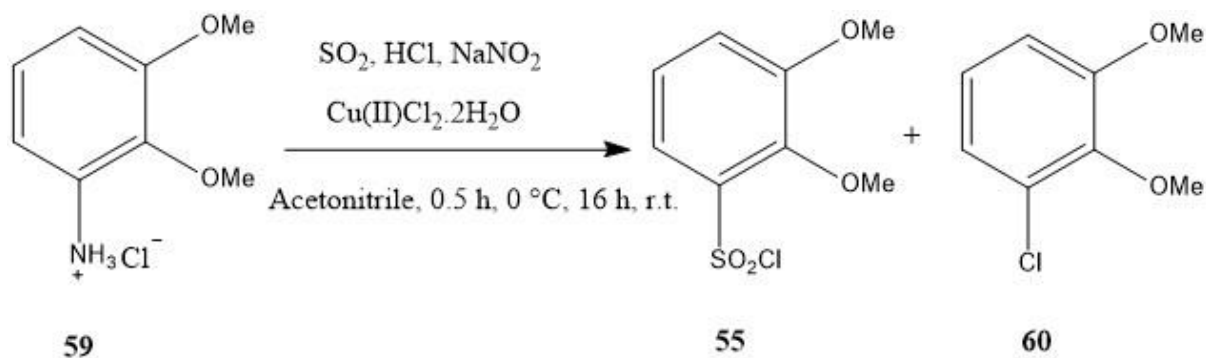
a



b

**Figure 8.** a)<sup>13</sup>C NMR spectrum and b)<sup>1</sup>H NMR spectrum of **59** in methanol-*d*<sub>4</sub>.

## 2.4 Synthesis of 2,3-dimethoxybenzenesulfonyl chloride (**55**)



**Scheme 15.** Synthesis of 2,3-dimethoxybenzenesulfonyl chloride **55** and unwanted side product 1-chloro-2,3-dimethoxybenzene **60**.

The synthesis of sulfonyl chloride **55** was achieved from the amine salt **59** by way of a diazonium salt **61** (figure 9) following Meerwein's classic procedure.<sup>29</sup> We believed that generation of **61** in the presence of  $\text{SO}_2$  and a catalytic quantity of  $\text{CuCl}_2$ <sup>28</sup> would afford **55**. A modification to the method was made by reducing the time that the reaction was exposed to

SO<sub>2</sub> from two hours to 30 mins. The change was made in light of finding out that sulfur dioxide had a high solubility coefficient in acetonitrile (84.6g/100g)<sup>30</sup>. This meant that even after 30 minutes the acetonitrile solvent system should be fully saturated. Purification of the compound was achieved using column chromatography; ethyl acetate: petroleum ether 1:40 was used as the eluent, and a colourless crystalline solid was afforded in 76% yield. <sup>1</sup>H and <sup>13</sup>C NMR spectroscopy of **55** confirmed the presence of 5 distinct proton environments and 8 carbon environments. Melting point analysis results were consistent with literature value. HRMS and elemental microanalysis data confirmed that the sulfonyl chloride **55** had been successfully synthesised.

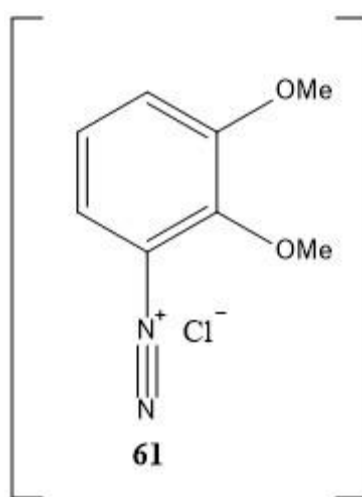
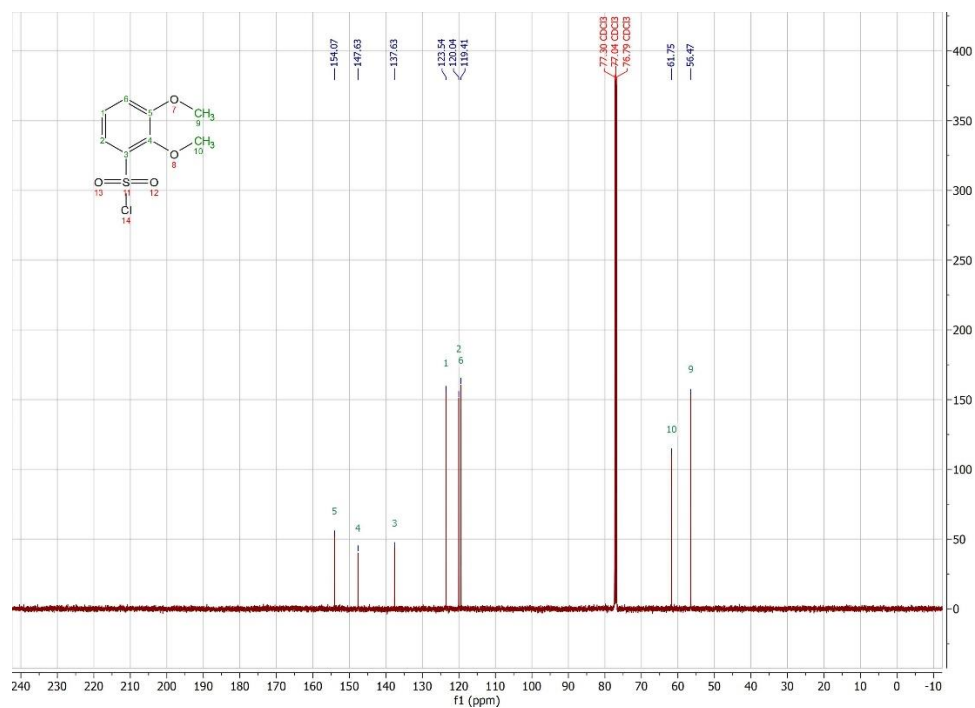


**Figure 9.** diazonium **61**.

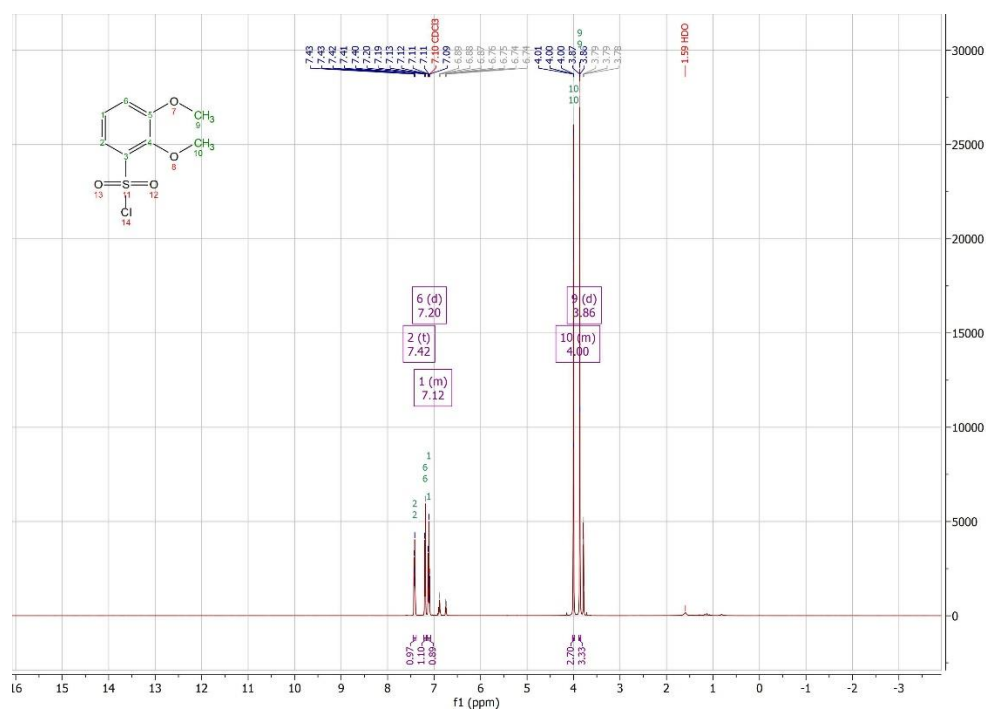
On a subsequent attempt at the synthesis the sulfur dioxide was only bubbled through the reaction mixture for 5 minutes due to a shortage of the gas. Once purification had been completed a colourless crystalline solid was again obtained albeit in lower yield (45%). On this occasion the formation of **55** was accompanied by isolation of a second, non-polar, product a pale yellow oil. Initially unsure as to what the side product obtained was, a study was found that elucidated the identity of the unwanted side product.<sup>31</sup> The side product was found to be 1-chloro-2,3-dimethoxybenzene **60**. This was the substitution product of the diazonium salt when there was a lack of SO<sub>2</sub> in the solvent system with chloride reacting instead. The identity of the side product was confirmed using **HRMS** for C<sub>8</sub>H<sub>9</sub><sup>35</sup>ClO<sub>2</sub>H (MH<sup>+</sup>) (expected mass: 173.0364; actual mass: 173.064), <sup>1</sup>H and <sup>13</sup>C NMR spectroscopy (figure 11). The modification



to the reaction did not hinder the yield obtained so allowed for more efficient use of SO<sub>2</sub> which would be important on larger scales and allows more reactions to be run for less expenditure.

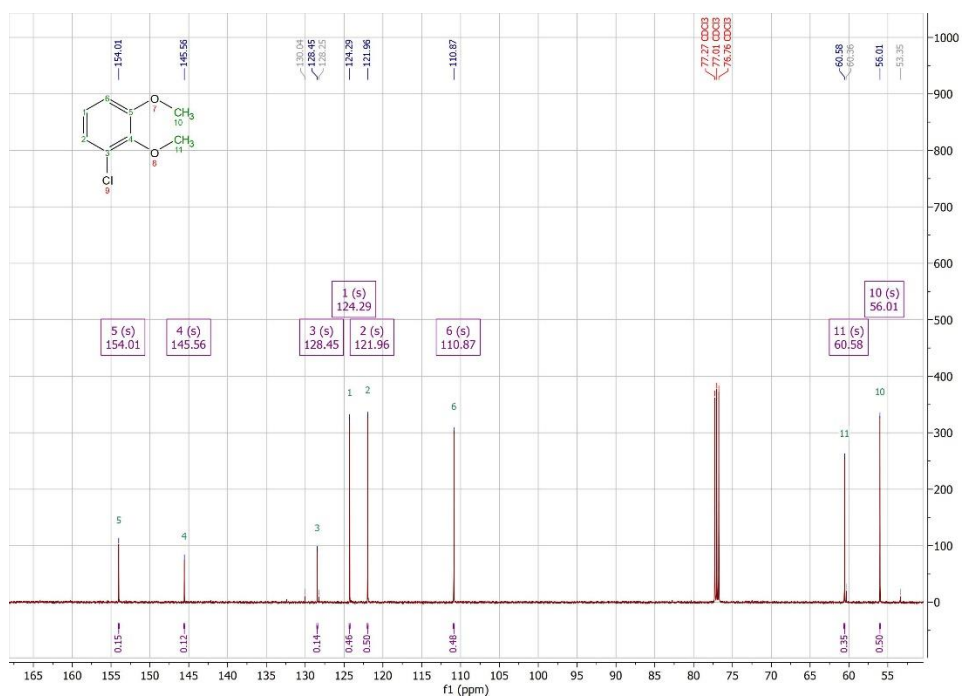


a

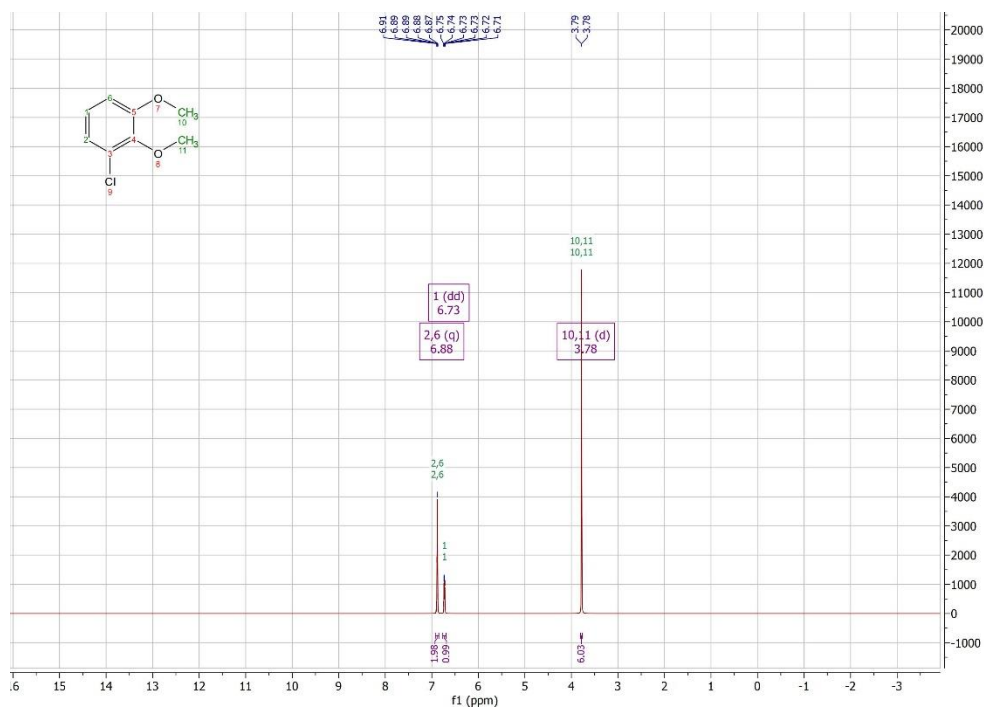


b

**Figure 10.** a)<sup>13</sup>C NMR spectrum and b)<sup>1</sup>H NMR spectrum of **55** in chloroform-*d*.



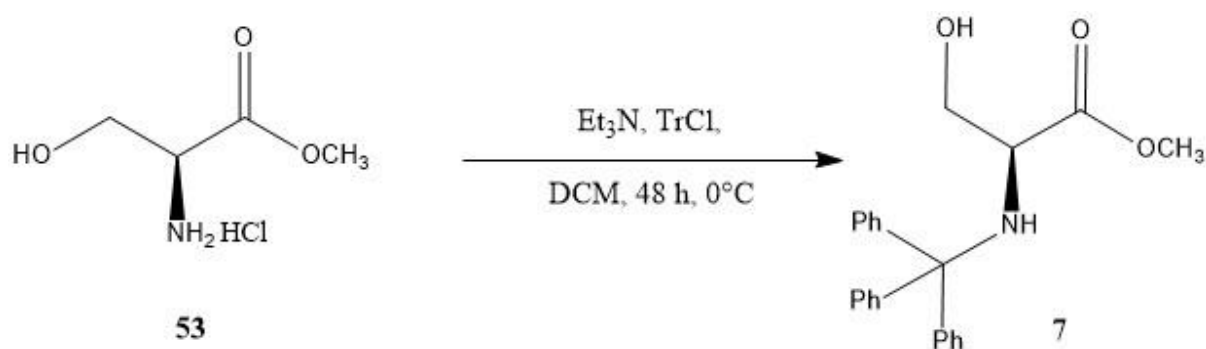
a



b

**Figure 11.** a) <sup>13</sup>C NMR spectrum and b) <sup>1</sup>H NMR spectrum of **60** in chloroform-*d*

## 2.5 Synthesis of Methyl trityl-L-serinate (**7**)



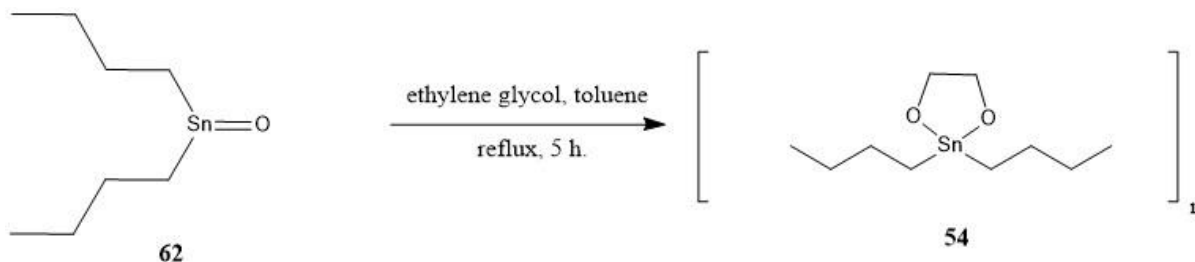
**Scheme 16.** Synthesis of methyl trityl-L-serinate **7**.

Methyl trityl L-serinate, **7** was obtained from the reaction of L-serine methyl ester hydrochloride **53** and trityl chloride (TrCl) in the presence of triethylamine (Et<sub>3</sub>N) in dichloromethane (DCM) for 48 hours. Gratifyingly, work-up and recrystallization (ethyl acetate and hexane; 1:1 v/v) of this reaction product afforded **7** as a colourless crystalline solid (84% yield). Melting point analysis revealed a value higher than literature value which suggested a pure product was obtained. <sup>1</sup>H NMR and <sup>13</sup>C NMR spectra showed the presence of 8 proton environments and 12 distinct carbon environments. MS showed a mass peak of 384 ([M + Na]<sup>+</sup>) expected for the formula of **7** C<sub>23</sub>H<sub>23</sub>NO<sub>3</sub>. HRMS and elemental microanalysis also confirmed that the crystalline solid obtained was indeed **7**.

A challenging aspect of the synthesis was to maintain the temperature of the reaction vessel at 0 °C which was achieved using an ice/methanol bath that was changed regularly to maintain the temperature. Another finding was that the crude form of **7** was incredibly hard to remove from the reaction vessel due to the adhesive property of it which was due to impurities. Recrystallisation was employed to overcome the issue as well as for a purer product.

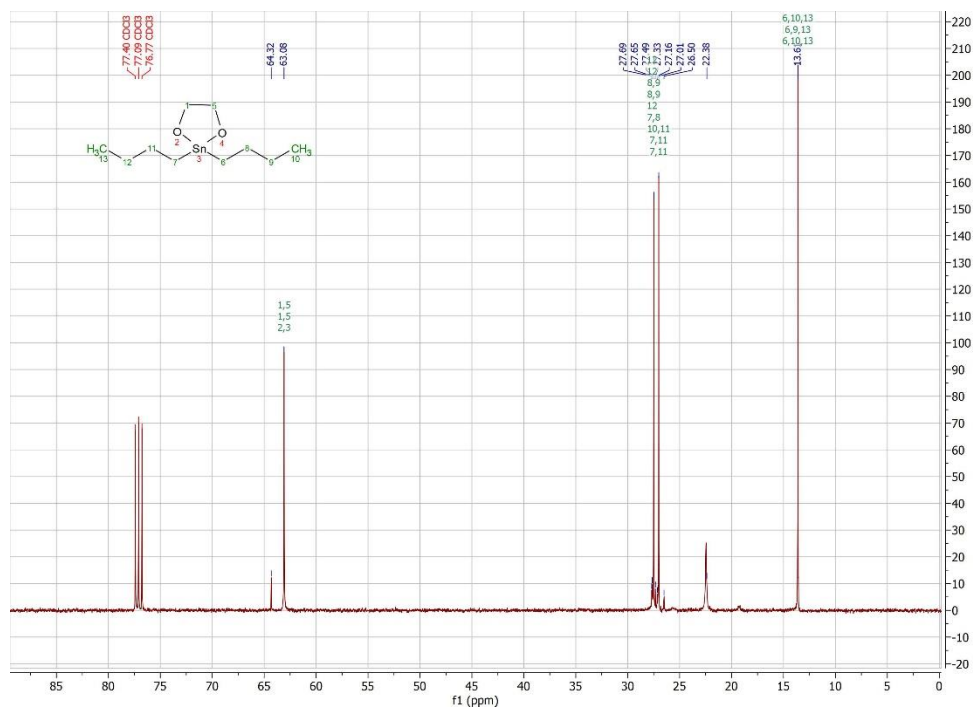


## 2.6 Synthesis of 2,2-dibutyl-1,3,2-dioxastannolane (**54**)

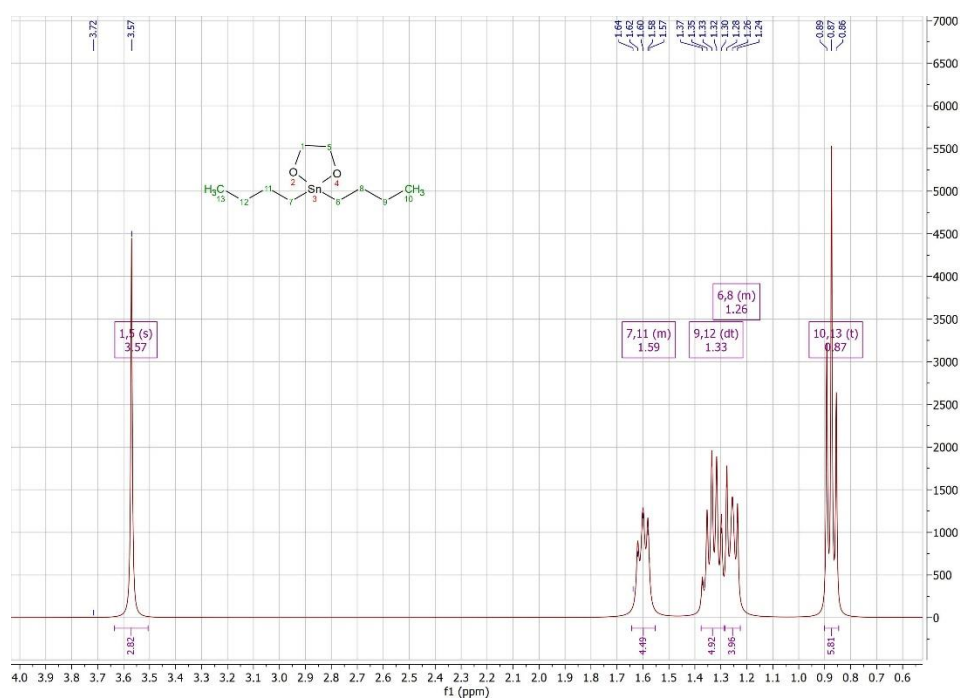


**Scheme 17.** Synthesis of 2,2-dibutyl-1,3,2-dioxastannolane **54**.

The dioxastannolane **54** which exists in an oligomeric form was required for the trimerization of **7** to **8**. Although commercially available there was a long delivery delay and we decided therefore to employ a well tried synthetic route<sup>32</sup> for its preparation starting with dibutyltin(IV) oxide **62**. Firstly **54** was refluxed for five hours with ethylene glycol in toluene using a Dean-Stark trap for the removal of water that was generated during the reaction. After filtration the solid filtrate obtained was recrystallised from toluene to afford **54** in an 83% yield. NMR analysis of **54** confirmed the presence of 5 distinct proton environments and 5 carbon environments. The obtained product was proven to be pure as the melting point recorded was above that of the literature value. HRMS and elemental analysis confirmed that the crystalline solid obtained was indeed dioxastannolane **54**.



a



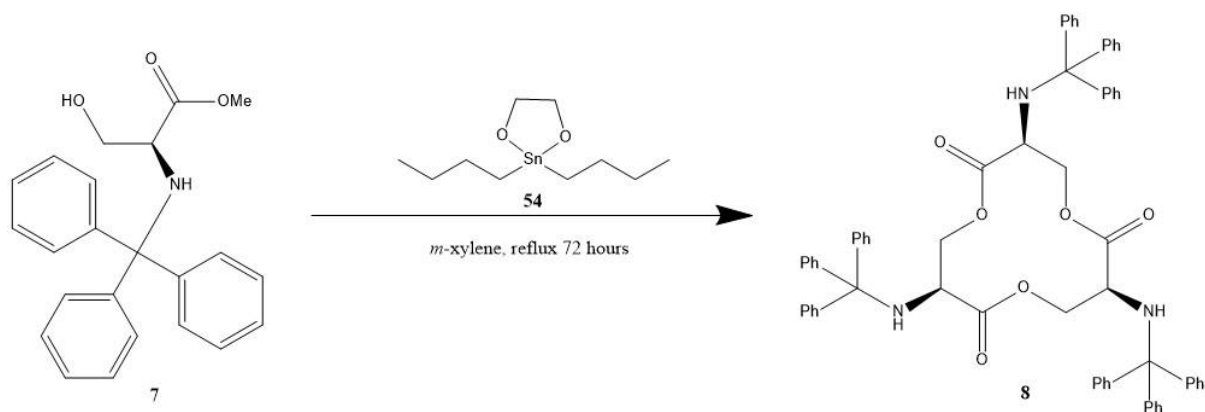
b

**Figure 13.** a)  $^{13}\text{C}$  NMR spectrum and b)  $^1\text{H}$  NMR spectrum of **54** in chloroform-*d*

The one step synthesis was straightforward and allowed for cheap starting material to be used so was easily scalable. The recrystallisation gave fine crystals which were needed for the next

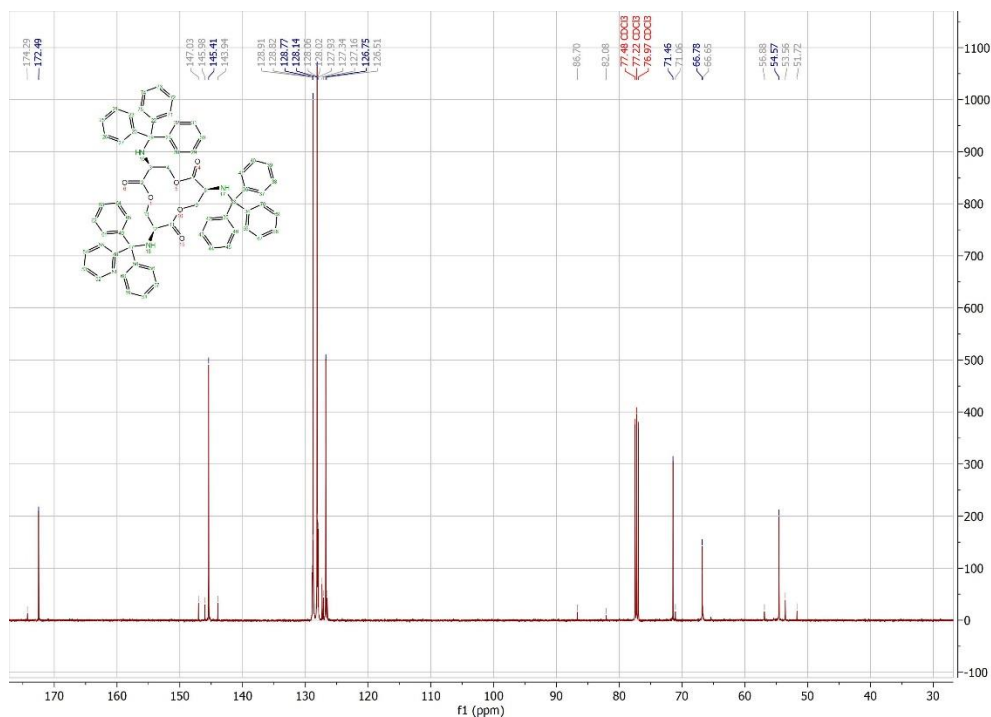
step of the overall synthesis (formation of trilactonate ring **8**). As only a catalytic amount of **54** was needed for the next step, the synthesis did not need to be repeated many times.

## 2.7. Synthesis of (3S,7S,11S)-3,7,11-tris(tritylamino)-1,5,9-trioxacyclododecane-2,6,10-trione (**8**)

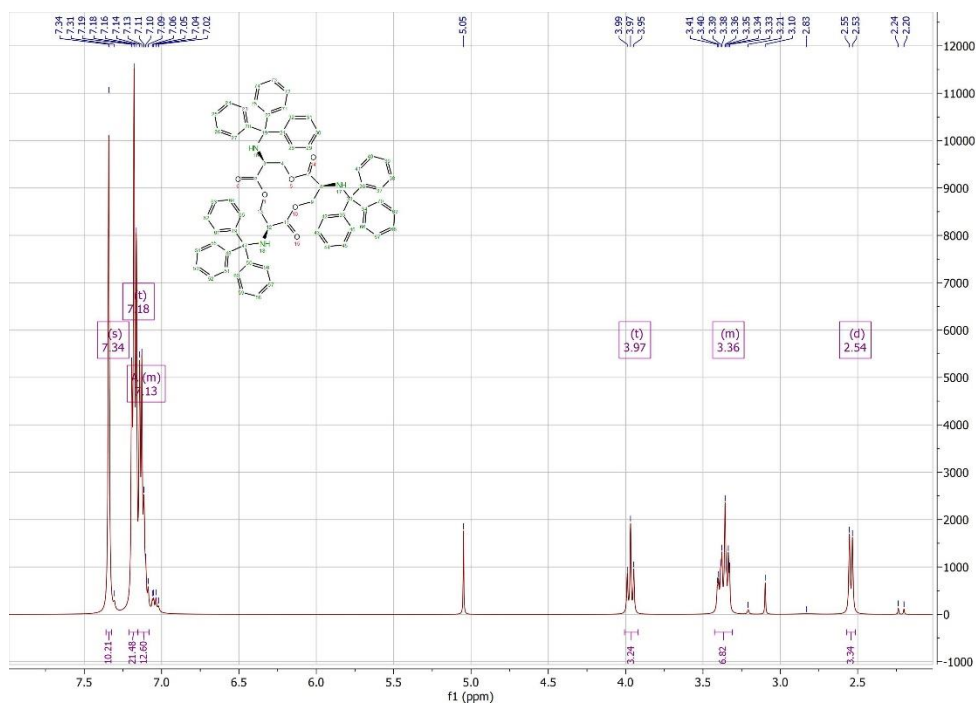


**Scheme 18.** Synthesis of (3S,7S,11S)-3,7,11-tris(tritylamino)-1,5,9-trioxacyclododecane-2,6,10-trione **8**

The next step of the synthetic route detailed in scheme 11 was trimerization of **7** in the presence of 2,2-dibutyl-1,3,2-dioxastannolane **54** (0.1 equivalents) in *m*-xylene for 72 hours using a Soxhlet apparatus to remove methanol with molecular sieves. On completion of work-up and subsequent removal of solvent the crude was purified using column chromatography with a dichloromethane as solvent system. Solid obtained was then recrystallised using a 1:1 mixture of DCM and hexane to afford **8** as a colourless crystalline solid (86%). NMR analysis of **8** confirmed the presence of 5 distinct proton environments and 8 carbon environments. MS showed a mass peak in the mass spectrum at 1011 ( $[M+Na]^+$ ). HRMS was run and the result obtained (mass required for  $C_{66}H_{57}N_3O_6$  1010.4140; actual mass found 1010.4143) indicated that the product had the correct constitution corresponding to **8**.



a



b

**Figure 14.** a) <sup>13</sup>C NMR spectrum and b) <sup>1</sup>H NMR spectrum of **8** in chloroform-*d*

There were few important points to note on the synthesis. Firstly, it was very important that the starting materials **7** and **54** were dry before reaction was commenced as there were multiple failed attempts without drying of the reagents. The Soxhlet apparatus that was used had to be



loaded with activated molecular sieves as there were various failed attempts due to improper removal of methanol and water from the reaction mixture. The reaction was attempted in toluene but because it had a lower boiling point than *m*-xylene therefore refluxed at a lower temperature. The attempts made at using it all failed to synthesise trilactonate **8**. All failed attempts resulted in the generation of a mixture of products, including **8** and oligomers of the starting material **7**. The mixture of products could not be purified sufficiently to obtain a pure yield of **8**. A timeframe of 72 hours was used for the synthesis of **8** using *m*-xylene instead of the suggested 96 found in literature<sup>26</sup> due to the multiple attempts that were made to find the optimal conditions (experimental section) for the synthesis to be robust and work successfully in a limited timeframe.

### 3. Conclusion

The aims of the research were to synthesise enterochelin analogue **52** following a post functionalisation approach and to test the analogue as a conjugate for an antibiotic delivery system. Steps of the synthesis were completed, and intermediates were successfully obtained however the full reaction series was not completed. Overall the synthetic route to enterochelin analogue **52** was not completed thus further testing as a conjugate could also not take place. Due to the initial difficulty in finding a reliable method for synthesis of trilactone **8** and time restraints the overall aim of the project was not met. However, improvements to the synthetic pathway to **52** were achieved. Recrystallisation of trityl serinate **7** and dioxastannolane **54** allowed for better quality of reagents for the trimerization step of the synthesis. A synthesis for HCl salt **59** has been developed that is one step and allows for good yields in a short time frame with minimal purification required. It has shown to be an up scalable method (up to 40 mmol) without sacrificing yield. Adaptations have been made to make synthesis of sulfonyl chloride **55** to be potentially less resource heavy and more cost effective. The saving could be tested by comparing cost and quantities of starting material used to make sulfonyl chloride **55** and the yield of both methods to determine the cost versus yield and get a quantifiable result. Finally, a reliable method has been detailed for the synthesis of trilactone **8**.

## 4. Future work

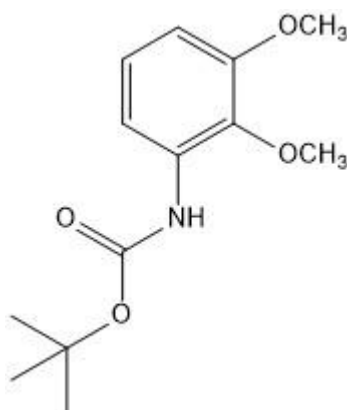
The first step of any future work carried out would be to complete the synthetic route to analogue **52** (scheme 11). Once this had been established large scale synthesis of the chelator should be carried out to obtain it gram scale. Biological activity of **52** as an iron (III) chelator should be tested and quantified by measuring its iron (III) binding constant to test the analogue's affinity. If positive results for biological activity are achieved **52** could be tested for its efficacy as a siderophore conjugate by attaching to antibiotics. It could be used as a trojan horse delivery system to allow for more effective antibiotic uptake by microbial pathogens. Another avenue of investigation could be the use of **52** as a ferric sensor for the uptake of iron by bacteria if groups that can act as fluorescent sensors are grafted to it<sup>33</sup>.

## 5. Experimental

### 5.1 General experimental procedure:

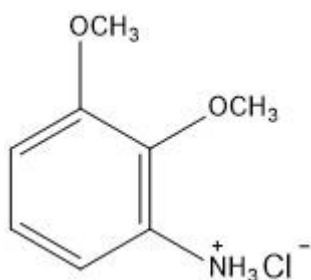
All reactions were conducted in dry glassware under a nitrogen atmosphere unless otherwise stated. All chemicals were purchased from Sigma-Aldrich, Fischer scientific and Fluorochem and used as received unless otherwise stated. Flash chromatography purifications were performed using technical grade silica gel (mesh 40-63  $\mu\text{m}$ , pore size 60Å 230-240).  $^1\text{H}$  NMR spectra were recorded at 400 or 500 MHz and  $^{13}\text{C}$  NMR spectra at 100 or 125 MHz on a Bruker AC400 or AC500 spectrometer. All NMR experiments were recorded using a standard 5 mm NMR tubes using deuterated solvents. The splitting patterns for NMR spectra are designated as follows: s (singlet), br.s (broad singlet), d (doublet), t (triplet), q (quartet), m (multiplet), or combinations. All the IR spectra obtained for these synthesized compounds were recorded using a Bruker Alpha FT-IR spectrometer or an ATI-Mattson Genesis Series or Perkin Elmer FT-IR spectrometer. Mass spectrometry analyses were recorded on either Waters QTOF (ES, HRMS) or Thermo Finnigan MAT95XP (GC/MS, EI, and HRMS) instruments. Melting points for all the compounds were recorded on a Sanyo Gallenkamp MPD350 heater. Analytical TLC was performed on Merck silica gel 60 F254 aluminium backed plates or Macherey-Nagel silica gel 60 UV254 polyester backed plates. The plates were visualised under UV light (254 nm)

## 5.2 Synthesis of tert-butyl (2,3-dimethoxyphenyl) carbamate (58)<sup>34</sup> :



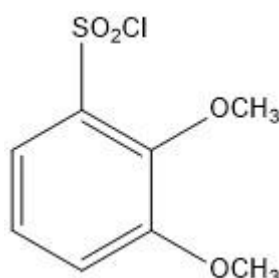
Et<sub>3</sub>N (8.8 ml; 63 mmol) and dried *t*-butanol (50 ml) were added to a solution of 2,3-dimethoxybenzoic acid (11.4 g 63 mmol) and DPPA (13.6 ml; 63.6 mmol) in 1,4-dioxane (120 ml). The reaction mixture was then refluxed for 16 hours and subsequently cooled to ambient temperature. Solvent was evaporated and residue obtained was dissolved in EtOAc (100 ml) which was washed with saturated Na<sub>2</sub>CO<sub>3</sub> (3 x 100 ml) and then brine (3 x 100 ml), dried (MgSO<sub>4</sub>) and concentrated *in vacuo*. Column chromatography of the residue [silica gel; EtOAc:pet. ether (40-60); 2:8 (v/v)] gave the *title compound* as a pale yellow coloured oil. Yield 9.6 g (60%). **IR**  $\nu_{\text{max}}$  (ATR) 3434 (w), 2977 (w), 1726 (m), 1604 (m), 1522 (m), 1480 (m), 1455 (m), 1416 (m), 1367 (w), 1298 (m), 1263 (s), 1083 (w), 998 (s), 778 (m), 735 (m) cm<sup>-1</sup>. **<sup>1</sup>H NMR** (500 MHz, chloroform-*d*)  $\delta$  7.72 (d, *J* = 7.9 Hz, 1H), 7.16 (s, 1H), 6.94 (t, *J* = 8.3 Hz, 1H), 6.53 (d, *J* = 8.3 Hz, 1H), 3.81 (s, 3H), 3.78 (s, 3H), 1.49 (s, 9H). **<sup>13</sup>C NMR** (126 MHz, chloroform-*d*)  $\delta$  152.6, 152.0, 136.9, 132.6, 124.0, 110.8, 106.2, 80.3, 60.4, 55.6, 28.2. **MS** (ES+) *m/z* 276 (C<sub>13</sub>H<sub>19</sub>NNaO<sub>4</sub>, [M+Na]<sup>+</sup>, 100%). **HRMS** (ES+) C<sub>13</sub>H<sub>19</sub>NO<sub>4</sub> [M+H]<sup>+</sup> requires *m/z* 254.1387, found 254.1386.

## 5.3 Synthesis of 2,3-dimethoxyaniline hydrochloride (59):



Tert-butyl (2,3-dimethoxyphenyl) carbamate (3.0g, 16 mmol) and 4 M HCl/dioxane (9.0 ml, 36 mmol) were refluxed for 30 minutes, the resulting solid was filtered and washed with cold diethyl ether (20 ml). The solid was dried under vacuum for 1 hour to afford the *title compound* as a yellow coloured crystalline solid. Yield 1.85 g (82%); mp 210-212 °C (lit 177-178 °C)<sup>26</sup>. **IR**  $\nu_{\text{max}}$  (ATR) 2876 (s), 2587 (m), 1559 (m), 1475 (s), 1289 (s), 993 (s)  $\text{cm}^{-1}$ . **<sup>1</sup>H NMR** (400 MHz, methanol-*d*<sub>4</sub>)  $\delta$  7.24 – 7.13 (m, 2H), 7.01 (dd, *J* = 6.5, 3.0 Hz, 1H), 4.01 (s, 3H), 3.94 (s, 3H). **<sup>13</sup>C NMR** (101 MHz, methanol-*d*<sub>4</sub>)  $\delta$  153.2, 142.5, 124.2, 114.9, 113.4, 60.4, 55.3. **MS** (ES+) *m/z* 154 (C<sub>18</sub>H<sub>12</sub>NO<sub>2</sub>, [M+H]<sup>+</sup>, 95%). **HRMS** (ES+) C<sub>18</sub>H<sub>12</sub>NO<sub>2</sub> [M+H]<sup>+</sup> requires *m/z* 154.0863, found 154.0858. **Microanalysis** C<sub>8</sub>H<sub>12</sub>ClNO<sub>2</sub> requires C 50.66, H 6.33, N 7.39, Cl 18.73%; found C 50.83, H 6.40, N 7.32, Cl 18.59 %.

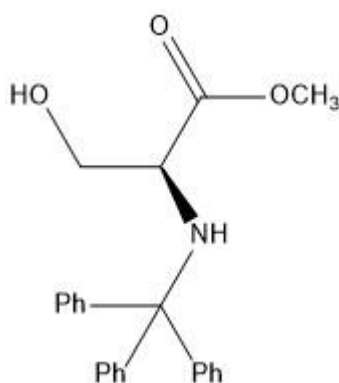
#### 5.4 Synthesis of 2,3-dimethoxybenzenesulfonyl chloride (55)<sup>28</sup> :



To acetonitrile (250 ml) a solution of 2,3-dimethoxyaniline hydrochloride (3.9 g, 21 mmol) in acetic acid (12 ml) and concentrated HCl (13 ml /11M solution) were added and the resulting mixture was cooled to 0 °C using a ice bath. Sodium nitrite (2.0g, 29 mmol) in distilled water (5 ml) was added slowly over the course of 5 minutes. On completion of addition the reaction mixture was stirred at 0 °C for 30 minutes. SO<sub>2</sub> was then bubbled through the mixture for 30 minutes at 0 °C and copper(II) chloride dihydrate (4.8 g, 28 mmol) was added while maintaining the flow of SO<sub>2</sub>. After the addition was complete the reaction mixture was then stirred at 0°C for a further 1 hour and then 16 hours at ambient temperate. The reaction mixture was poured into ice-cold water (400 ml) and extracted using DCM (3x 300 ml). The organic layers were combined, washed (brine, 3x 200ml), dried (MgSO<sub>4</sub>) and solvent was removed. The residue was purified using column chromatography [silica gel; EtOAc: pet ether (40-60), 1:40 v/v] which afforded the *title compound* as a colourless crystalline solid. Yield 3.7 g (76%);

**mp** 70-73 °C (lit<sup>26</sup> 71-73 °C). **IR**  $\nu_{\max}$  (ATR) 2842 (w), 1583 (w), 1483 (s), 1363 (s), 1173 (s)  $\text{cm}^{-1}$ . **<sup>1</sup>H NMR** (500 MHz, chloroform-*d*)  $\delta$  7.42 (t, *J* = 6.5 Hz, 1H), 7.20 (d, *J* = 8.1 Hz, 1H), 7.15 – 7.07 (m, 1H), 4.02 – 3.98 (m, 3H), 3.86 (d, *J* = 2.9 Hz, 3H). **<sup>13</sup>C NMR** (126 MHz, chloroform-*d*)  $\delta$  154.1, 147.6, 137.6, 123.5, 120.0, 119.4, 61.8, 56.5. **MS** (ES+) *m/z* 259 ( $\text{C}_8\text{H}_9^{35}\text{ClNaO}_4\text{S}$ ,  $[\text{M}+\text{Na}]^+$ , 100%). **HRMS** (ES+)  $\text{C}_8\text{H}_9^{35}\text{ClO}_4\text{S}$ ,  $[\text{M}+\text{H}]^+$  requires *m/z* 236.9983, found 236.9982. **Microanalysis**  $\text{C}_8\text{H}_9\text{ClO}_4\text{S}$  requires C 40.60, H 3.83, Cl 14.98, S 13.55%; found C 40.36, H 3.78, Cl 15.25, S 13.21%.

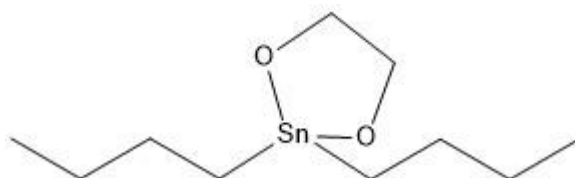
### 5.5 Synthesis of methyl trityl-L-serinate (7)<sup>35</sup> :



In a round bottom flask, a solution of  $\text{Et}_3\text{N}$  (21.6 ml, 151 mmol) and L-serine methyl ester hydrochloride (12.0 g, 77 mmol) in DCM (32 ml) was cooled to 0°C. Trityl chloride (22.0 g, 79 mmol) dissolved in DCM (48 ml) was then added to the flask. The resulting mixture was then stirred for 48 hours at 0°C and then washed with citric acid 10% solution (72 ml), brine (72 ml) and subsequently dried with  $\text{MgSO}_4$ . DCM was removed via rotary evaporation and the solid obtained was then recrystallised using ethyl acetate and hexane (1:1) to obtain methyl trityl-L-serinate as a colourless, crystalline, solid. Yield 23.4 g (84%); **mp** 144-145 °C (lit<sup>35</sup> 138 °C). **IR**  $\nu_{\max}$  (ATR) 3450 (m), 3350 (w), 1702 (s), 1055 (m)  $\text{cm}^{-1}$ . **<sup>1</sup>H NMR** (500 MHz,  $\text{CDCl}_3$ )  $\delta$  7.57 – 7.51 (m, 6H), 7.31 (t, *J* = 7.7 Hz, 6H), 7.23 (t, *J* = 7.3 Hz, 3H), 3.76 (dd, *J* = 10.6, 4.5 Hz, 1H), 3.62 (dd, *J* = 10.6, 5.6 Hz, 1H), 3.61 – 3.55 (m, 1H), 3.33 (s, 3H), 2.97 (s, 1H), 2.51 (s, 1H). **<sup>13</sup>C NMR** (126 MHz,  $\text{CDCl}_3$ )  $\delta$  174.0, 145.7, 128.8, 128.0, 126.7, 71.0, 65.0, 57.9, 52.0. **MS** (ES+) *m/z* 384 ( $\text{C}_{23}\text{H}_{23}\text{NNaO}_3$ ,  $[\text{M}+\text{Na}]^+$ , 100%). **HRMS** (ES+)  $\text{C}_{23}\text{H}_{23}\text{NO}_3$   $[\text{M}+\text{K}]^+$  requires *m/z* 400.1310, found 400.1295. **Microanalysis**  $\text{C}_{23}\text{H}_{23}\text{NO}_3$  requires C 76.43,

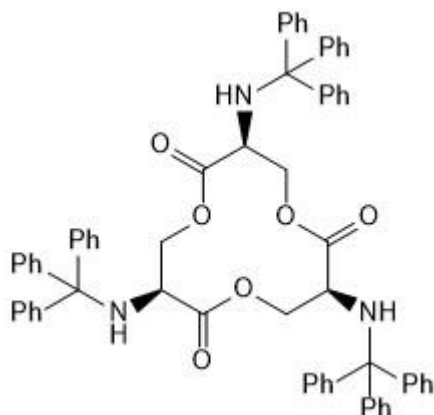
H 6.41, N 3.88%; found C 76.17, H 6.41, N 3.87%.  $[\alpha]_D^{28} +8.7$  (c. 1.0, DCM) (lit<sup>26</sup> +8.4 c. 1.0, DCM)

### 5.6 Synthesis of 2,2-dibutyl-1,3,2-dioxastannolane (54)<sup>32</sup> :



To a suspension of dibutyltin(IV) oxide (5.0 g, 20.2 mmol) in toluene (50 ml) ethylene glycol (5 ml, 90.3 mmol) was added. The reaction mixture was refluxed for 5 hours using a Dean-Stark trap for the removal of water generated during the reaction. After letting the reaction mixture cool to ambient temperature vacuum filtration was used to collect solid material and solvent was removed from filtrate via rotary evaporation. Solid obtained was combined and recrystallised from toluene and dried under vacuum to afford the *title compound* as a colourless, crystalline solid. Yield 4.9 g (83%); **mp** 231-234 °C (lit<sup>32</sup> 230-231 °C). **IR**  $\nu_{\max}$  (ATR) 2953 (s), 1455 (m), 1061 (s)  $\text{cm}^{-1}$ . **<sup>1</sup>H NMR** (400 MHz,  $\text{CDCl}_3$ )  $\delta$  3.57 (s, 3H), 1.64 – 1.56 (m, 4H), 1.32 – 1.34 (m, 5H), 1.28 – 1.23 (m, 4H), 0.87 (t,  $J = 7.3$  Hz, 6H). **<sup>13</sup>C NMR** (101 MHz,  $\text{CDCl}_3$ )  $\delta$  63.1, 27.7, 27.5, 27.0, 13.6. **MS** (ES+)  $m/z$  317 ( $\text{C}_{10}\text{H}_{22}\text{NaO}_2^{119}\text{Sn}$ ,  $[\text{M}+\text{Na}]^+$ , 100%). **HRMS** (ES+)  $\text{C}_{10}\text{H}_{23}\text{O}_2^{119}\text{Sn}$   $[\text{M}+\text{H}]^+$  requires 295.0715, found 295.0713. **Microanalysis**  $\text{C}_{10}\text{H}_{22}\text{O}_2^{119}\text{Sn}$  requires C 40.99, H 7.57%; found C 41.04, H 7.58%.

## 5.7 Synthesis of (3S,7S,11S)-3,7,11-tris(tritylamino)-1,5,9-trioxacyclododecane-2,6,10-trione (**8**)<sup>24,36</sup> :



Methyl trityl-L-serinate (5.0 g, 14 mmol) and 2,2-dibutyl-1,3,2-dioxastannolane (0.4 g, 1.5 mmol) were dried under vacuum overnight, they were then added to anhydrous m-xylene (350 ml) and the solution refluxed at 170 °C for 72 hours under N<sub>2</sub> using a Soxhlet apparatus equipped with a thimble containing activated 4 Å molecular sieves for the removal of methanol produced during the reaction. Reaction mixture was cooled to ambient temperature and concentrated in vacuo. The residue was then purified by column chromatography (silica; DCM only) and the filtrate was concentrated by rotary evaporation. The residue was then recrystallised using (DCM – hexane, 1:1 v/v) to afford the *title compound* as a colourless crystalline solid. Yield 3.97 g (86%); **mp** 279-281 °C (lit<sup>26</sup> 278-282 °C). **IR**  $\nu_{\text{max}}$  (ATR) 3450 (m), 1702 (s), 1593 (m) cm<sup>-1</sup>. **<sup>1</sup>H NMR** (500 MHz, chloroform-*d*)  $\delta$  7.34 (s, 10H), 7.18 (t, *J* = 7.6 Hz, 21H), 7.15-7.08 (m, 13H), 3.97 (t, *J* = 10.5 Hz, 3H), 3.43 – 3.31 (m, 7H), 2.54 (d, *J* = 9.9 Hz, 3H). **<sup>13</sup>C NMR** (126 MHz, chloroform-*d*)  $\delta$  172.5, 145.4, 128.8, 128.1, 126.8, 71.5, 66.8, 54.6. **MS** (ES+) *m/z* 1011 (C<sub>66</sub>H<sub>57</sub>N<sub>3</sub>NaO<sub>6</sub>, [M+Na]<sup>+</sup>, 80%), **HRMS** (ES+) C<sub>66</sub>H<sub>57</sub>N<sub>3</sub>O<sub>6</sub> [M+Na]<sup>+</sup> requires 1010.4140; found 1010.4143. [ $\alpha$ ]<sub>D</sub><sup>28</sup> +97.5 (c. 1.0, DCM) (lit<sup>26</sup> +98.0 c. 1.0, DCM)

## 6. References

- 1 R. C. Hider and X. Kong, *Nat. Prod. Rep.*, 2010, **27**, 637–657.
- 2 T. Řezanka, A. Palyzová and K. Sigler, *Folia Microbiol. (Praha)*, 2018, **63**, 569–579.
- 3 B. R. Wilson, A. R. Bogdan, M. Miyazawa, K. Hashimoto and Y. Tsuji, *Trends Mol. Med.*, 2016, **22**, 1077–1090.
- 4 E. J. Wilde, A. Hughes, E. V. Blagova, O. V. Moroz, R. P. Thomas, J. P. Turkenburg, D. J. Raines, A. K. Duhme-Klair and K. S. Wilson, *Sci. Rep.*, 2017, **7**, 1–14.
- 5 M. R. Seyedsayamdost, M. F. Traxler, S. L. Zheng, R. Kolter and J. Clardy, *J. Am. Chem. Soc.*, 2011, **133**, 11434–11437.
- 6 A. du Moulinet d’Hardemare, N. Alnaga, G. Serratrice and J. L. Pierre, *Bioorganic Med. Chem. Lett.*, 2008, **18**, 6476–6478.
- 7 M. Ghosh, P. A. Miller, U. Möllmann, W. D. Claypool, V. A. Schroeder, W. R. Wolter, M. Suckow, H. Yu, S. Li, W. Huang, J. Zajicek and M. J. Miller, *J. Med. Chem.*, 2017, **60**, 4577–4583.
- 8 M. Nakao, S. Tsuji, S. Kitaike and S. Sano, *Synth.*, 2016, **48**, 4149–4154.
- 9 D. G. Workman, M. Hunter, L. G. Dover and D. Tétard, *J. Inorg. Biochem.*, 2016, **160**, 49–58.
- 10 C. Y. Zamora, A. G. E. Madec, W. Neumann, E. M. Nolan and B. Imperiali, *Bioorganic Med. Chem.*, DOI: 10.1016/j.bmc.2018.04.030.
- 11 E. A. Dertz, J. Xu, A. Stintzi and K. N. Raymond, *J. Am. Chem. Soc.*, 2006, **128**, 22–23.
- 12 B. Li, N. Li, Y. Yue, X. Liu, Y. Huang, L. Gu and S. Xu, *Biochem. Biophys. Res. Commun.*, 2016, **478**, 1049–1053.
- 13 C. Kurth, H. Kage and M. Nett, *Org. Biomol. Chem.*, 2016, **14**, 8212–8227.
- 14 M. Saha, S. Sarkar, B. Sarkar, B. K. Sharma, S. Bhattacharjee and P. Tribedi, *Environ. Sci. Pollut. Res.*, 2016, **23**, 3984–3999.



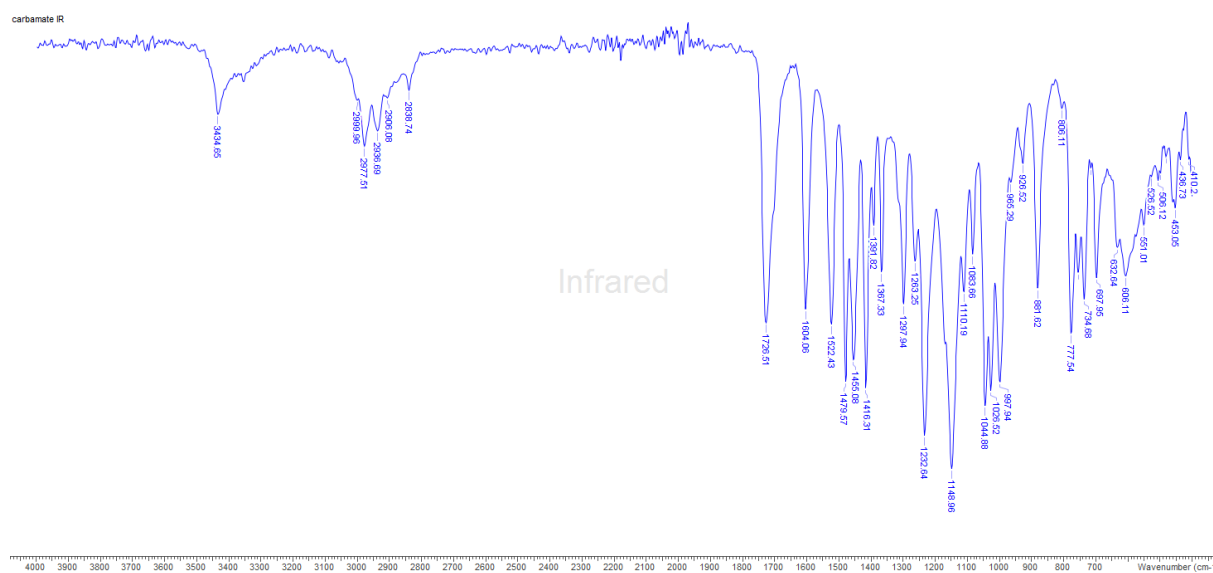
- 15 I. G. O'Brien and F. Gibson, *BBA - Gen. Subj.*, 1970, **215**, 393–402.
- 16 J. R. Pollack and J. B. Neilands, *Biochem. Biophys. Res. Commun.*, 1970, **38**, 989–992.
- 17 D. P. Frueh, H. Arthanari, A. Koglin, D. A. Vosburg, A. E. Bennett, C. T. Walsh and G. Wagner, *Nature*, 2008, **454**, 903–906.
- 18 E. . Corey and S. Bhattacharyya, *Tetrahedron Lett.*, 1977, 3919–3922.
- 19 W. H. Rastetter, T. J. Erickson and M. C. Venuti, *J. Org. Chem.*, 1980, **45**, 5011–5012.
- 20 K. N. Raymond, E. A. Dertz and S. S. Kim, *Proc. Natl. Acad. Sci.*, 2003, **100**, 3584–3588.
- 21 A. Shanzer and J. Libman, *J. Chem. Soc. Chem. Commun.*, 1983, 846–847.
- 22 A. Shanzer, J. Libman, S. Lifson and C. E. Felder, *J. Am. Chem. Soc.*, 1986, 7609–7619.
- 23 A. Akdeniz, M. G. Caglayan and P. Anzenbacher, *Chem. Commun.*, 2015, **52**, 1827–1830.
- 24 Y. Wang, E. Duran, D. Nacionales, A. Valencia, C. Wostenberg and E. R. Marinez, *Tetrahedron Lett.*, 2008, **49**, 6410–6412.
- 25 W. H. Rastetter, T. J. Erickson and M. C. Venuti, *J. Org. Chem.*, 1981, **46**, 3579–3590.
- 26 A.A. Bukhari, PhD thesis, University of Manchester, 2017.
- 27 Y. H. Ho, S. Y. Ho, C. C. Hsu, J. J. Shie and T. S. A. Wang, *Chem. Commun.*, 2017, **53**, 9265–9268.
- 28 WO 2010024980 A1 20100304, 2010.
- 29 P. J. Hogan and B. G. Cox, *Org. Process Res. Dev.*, 2009, 875–879.
- 30 J. J. Byerley, G. L. Rempel and V. Thang Le, *J. Chem. Eng. Data*, 1980, **25**, 55–56.
- 31 T. Wang, P. Rabe, C. A. Citron and J. S. Dickschat, *Beilstein J. Org. Chem.*, 2013, **9**, 2767–2777.
- 32 M. Guillaume and Y. Lang, *Tetrahedron Lett.*, 2010, **51**, 579–582.
- 33 T. Hayashi, A. Osawa, T. Watanabe, Y. Murata, A. Nakayama and K. Namba, *Tetrahedron Lett.*, 2017, **58**, 1961–1964.

- 34 L. Fumagalli, M. Pallavicini, R. Budriesi, C. Bolchi, M. Canovi, A. Chiarini, G. Chiodini, M. Gobbi, P. Laurino, M. Micucci, V. Straniero and E. Valoti, *J. Med. Chem.*, 2013, **56**, 6402–6412.
- 35 H. Liu, V. R. Pattabiraman and J. C. Vederas, *Org. Lett.*, 2007, **9**, 4211–4214.
- 36 A. Akdeniz, M. G. Caglayan and P. Anzenbacher, *Chem. Commun.*, 2015, **52**, 1827–1830.

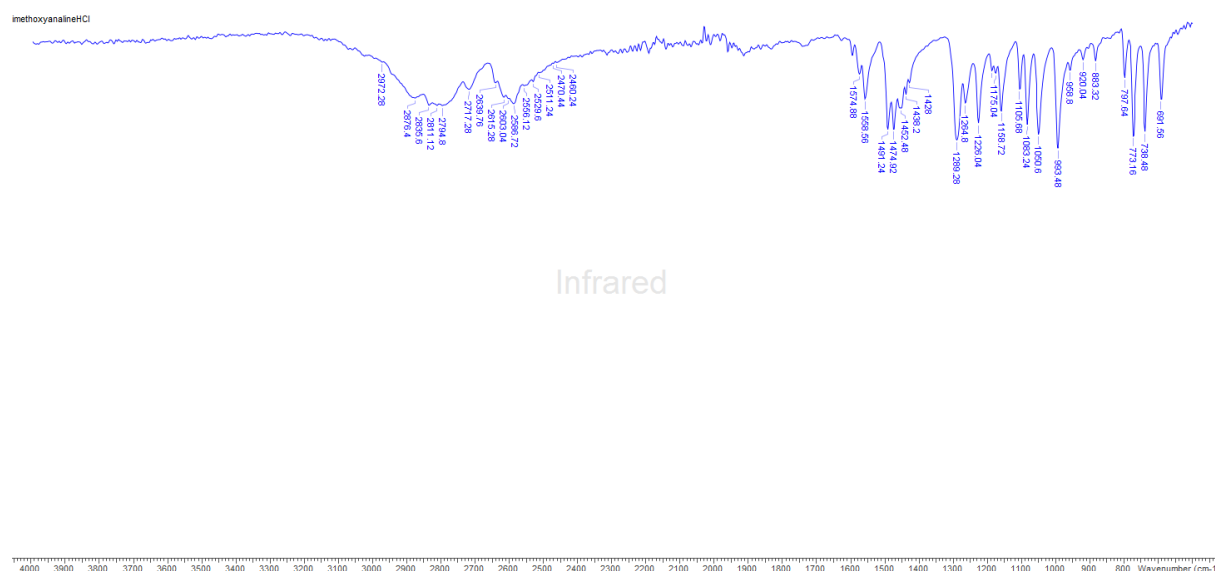
## 7. Appendix

### 7.1 Infra-red spectroscopic data

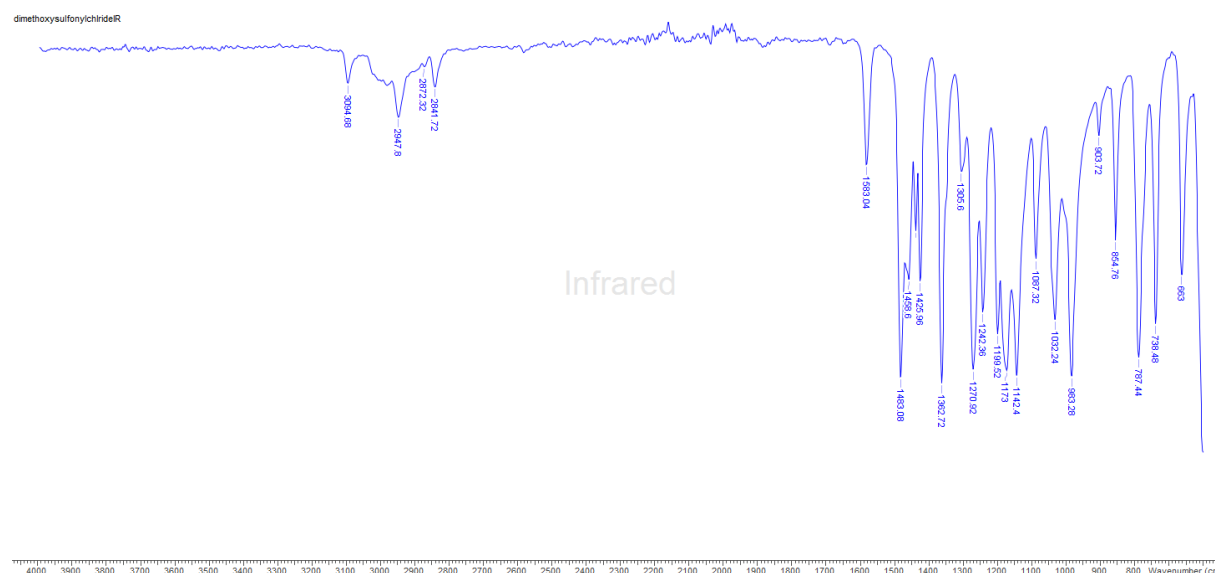
#### IR data for compound **58**



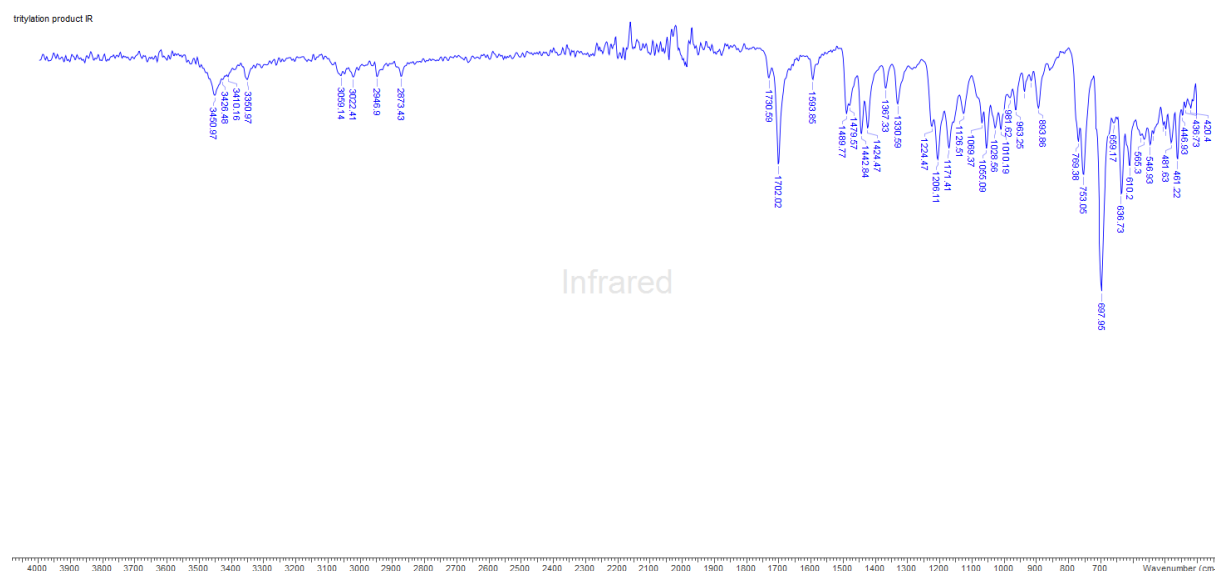
## IR data for compound **59**



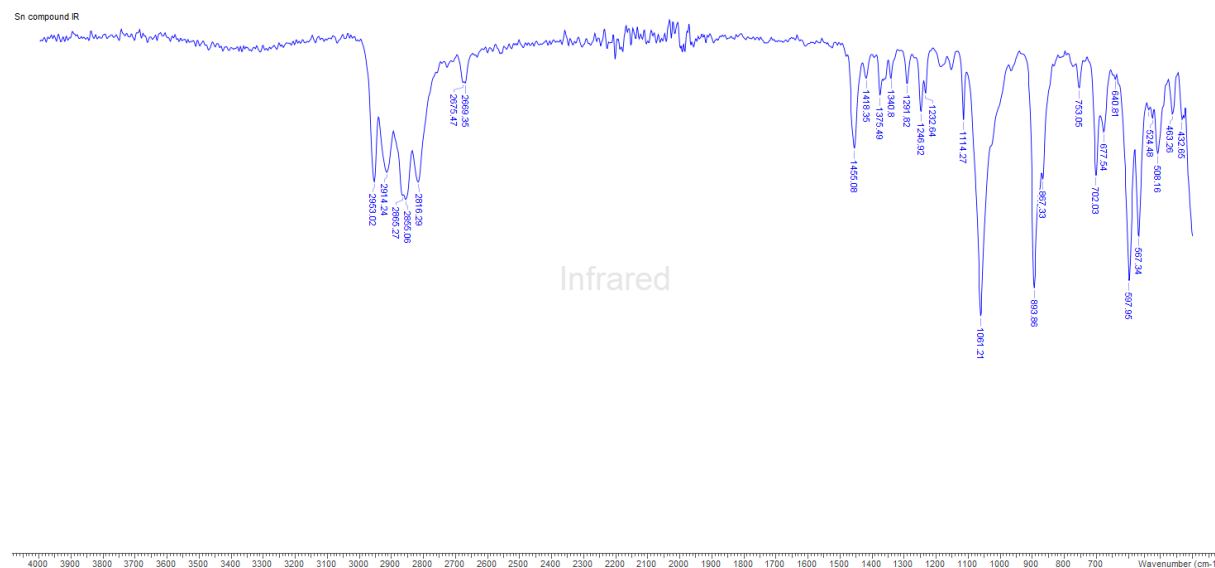
## IR data for compound **55**



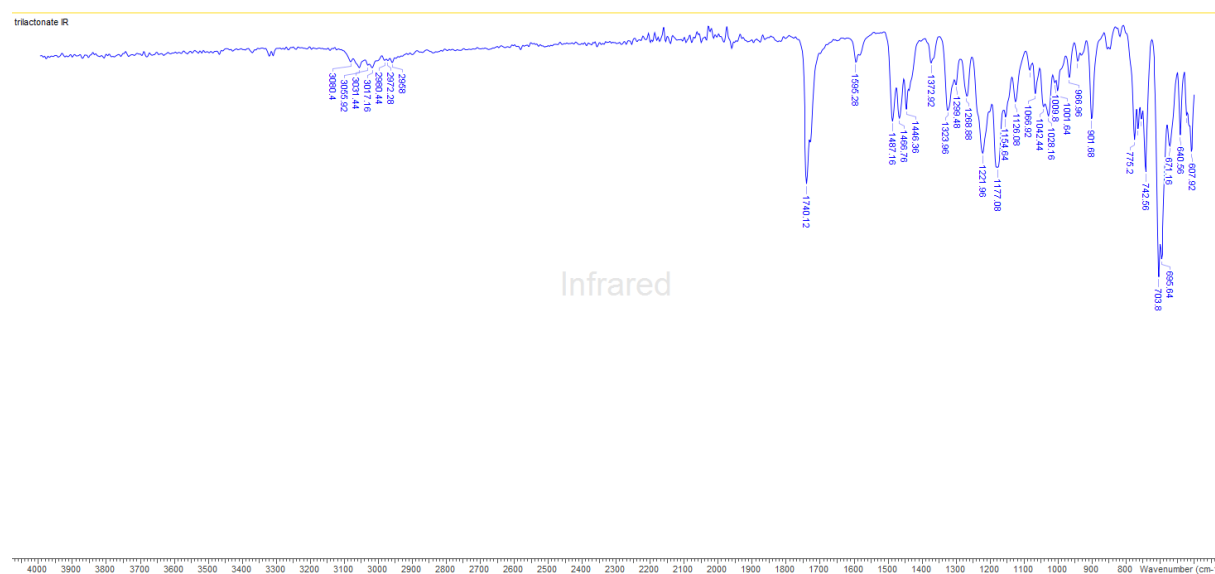
## IR data for compound **7**



## IR data for compound **54**

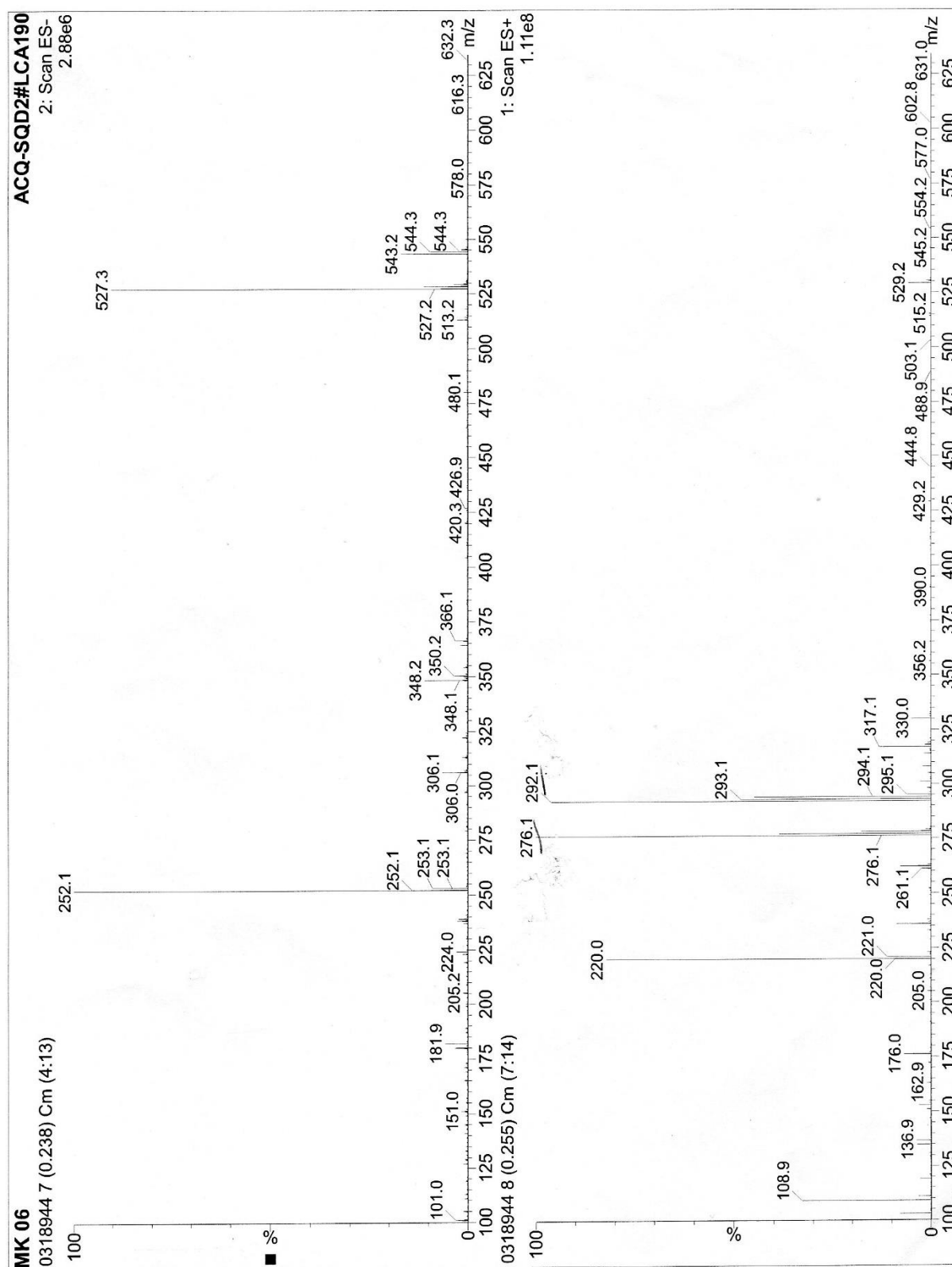


## IR data for compound **8**

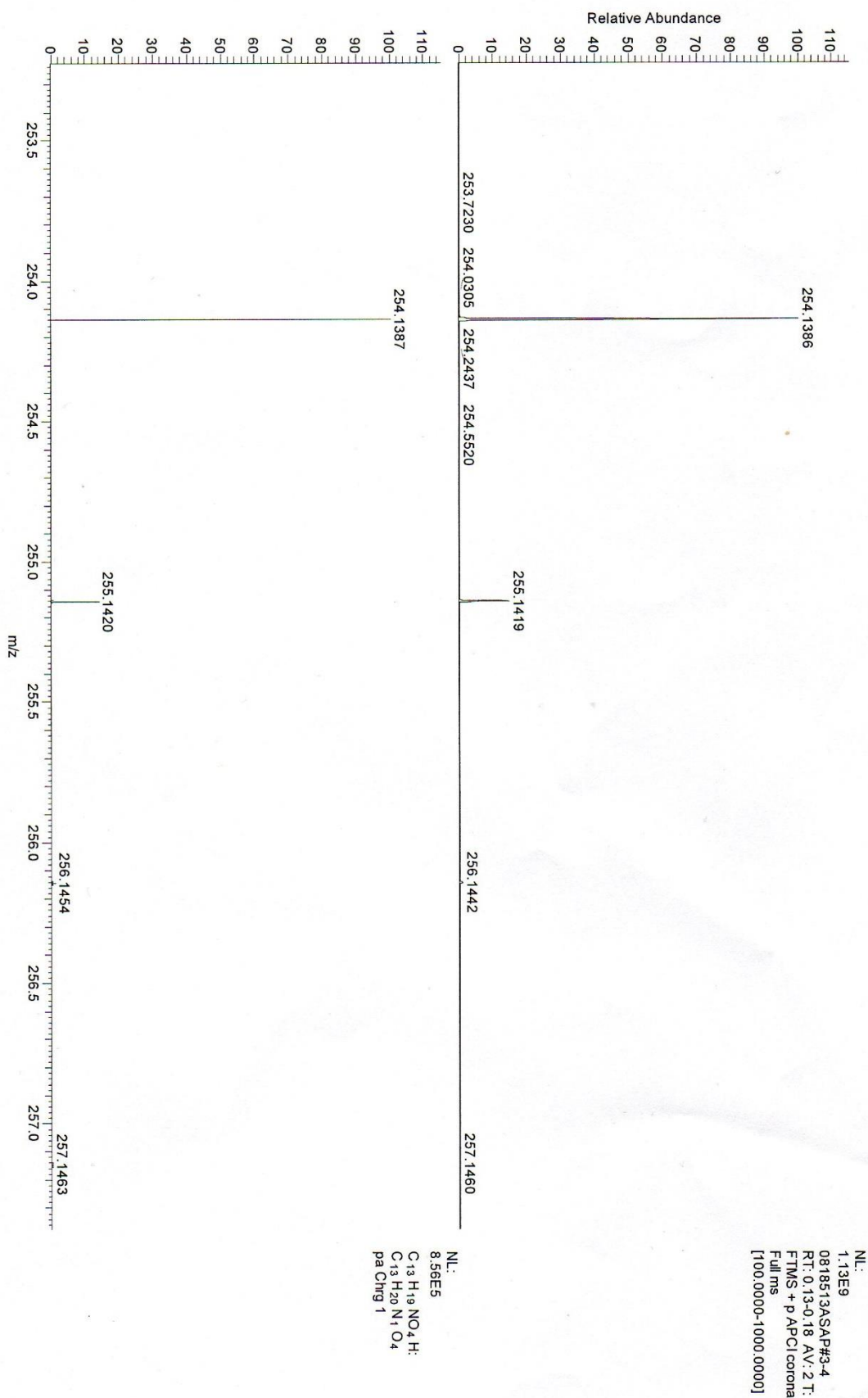


## 7.2 Mass Spectrometry Data

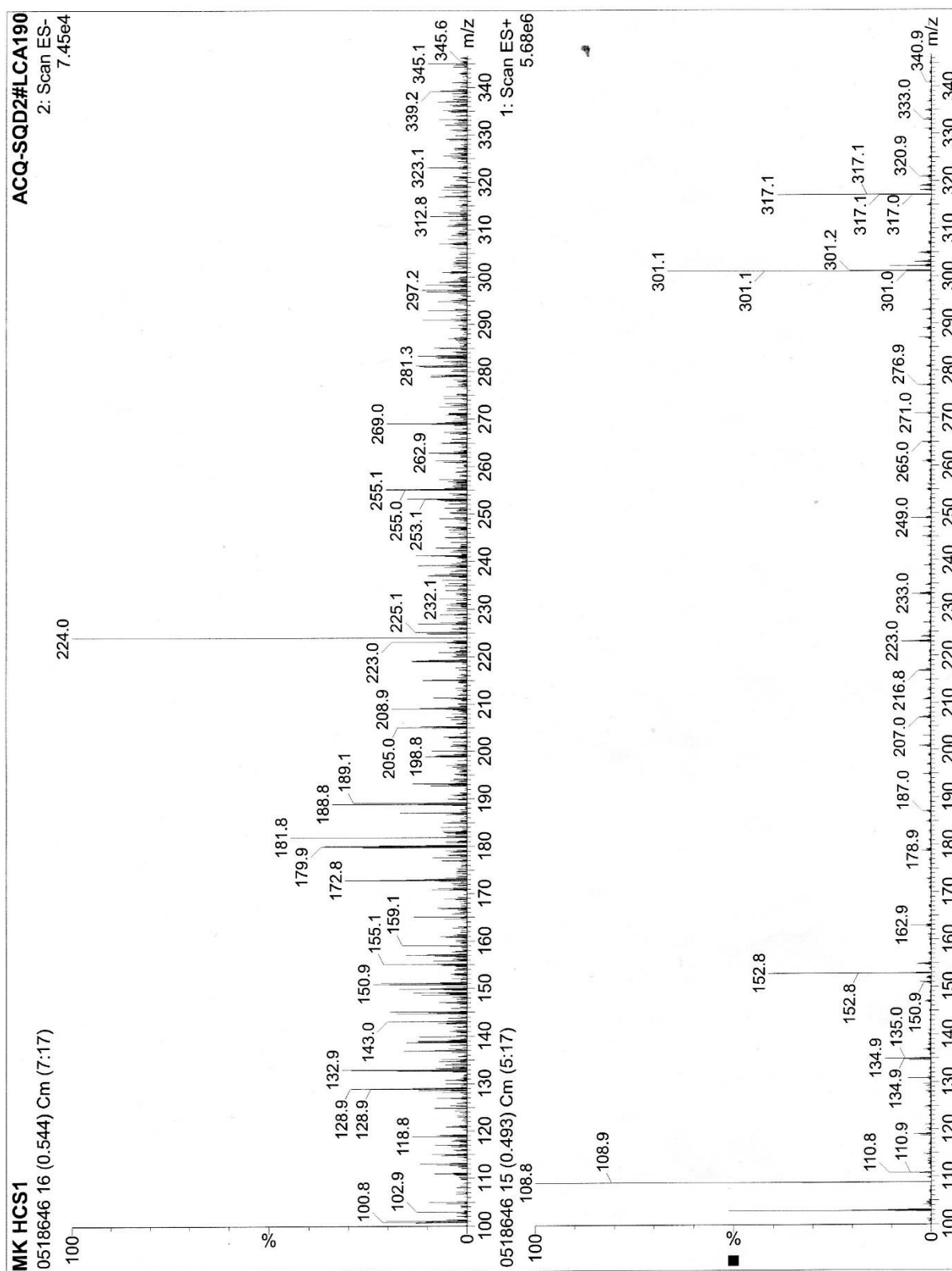
MS data for compound **58**



# Thermo Exactive Plus EMR Orbitrap ASAP pos



MS data for compound **59**

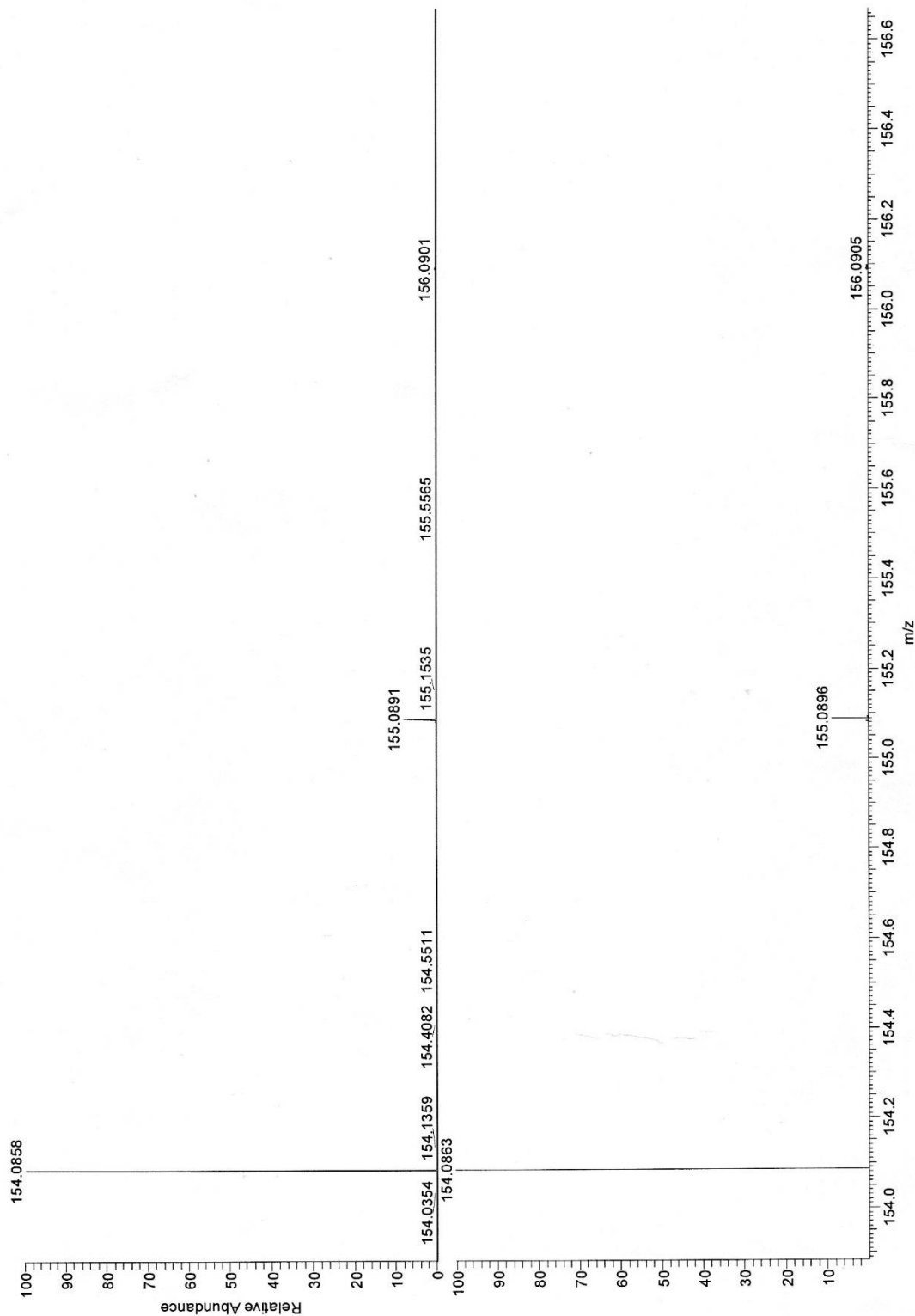




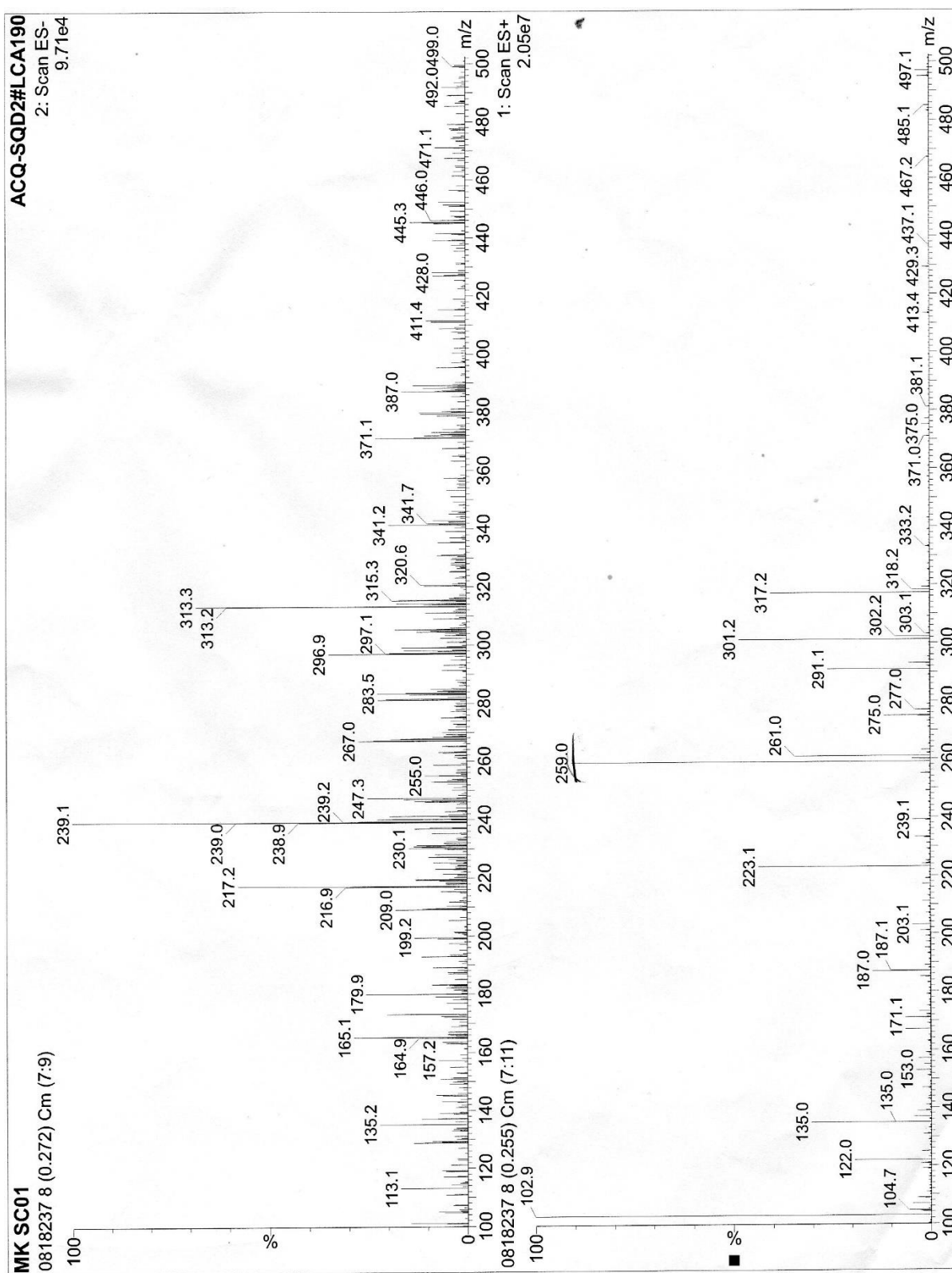
# Thermo Exactive Plus EMR Orbitrap ESI POS

NL:  
2.54E8  
0518857#15-18 RT:  
0.12-0.15 AV: 4 T:  
FTMS + p ESIFull  
ms  
[100.0000-  
1000.0000]

NL:  
9.08E5  
C<sub>8</sub>H<sub>12</sub>NO<sub>2</sub><sup>+</sup>  
C<sub>8</sub>H<sub>12</sub>N<sub>1</sub>O<sub>2</sub>  
pa Chg 1

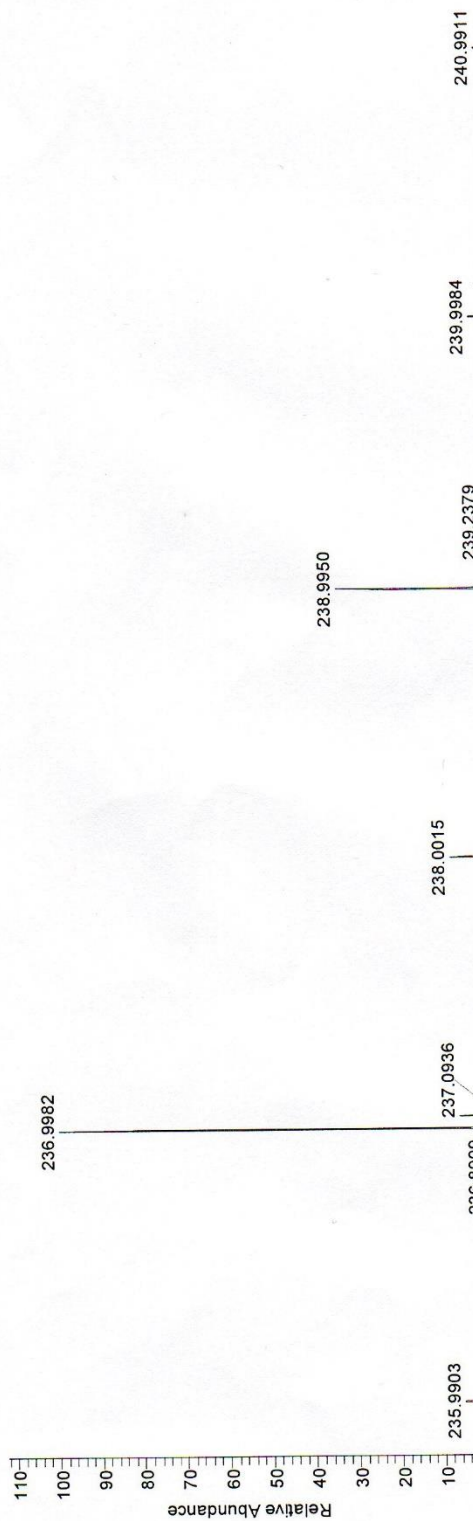


MS data for compound **55**

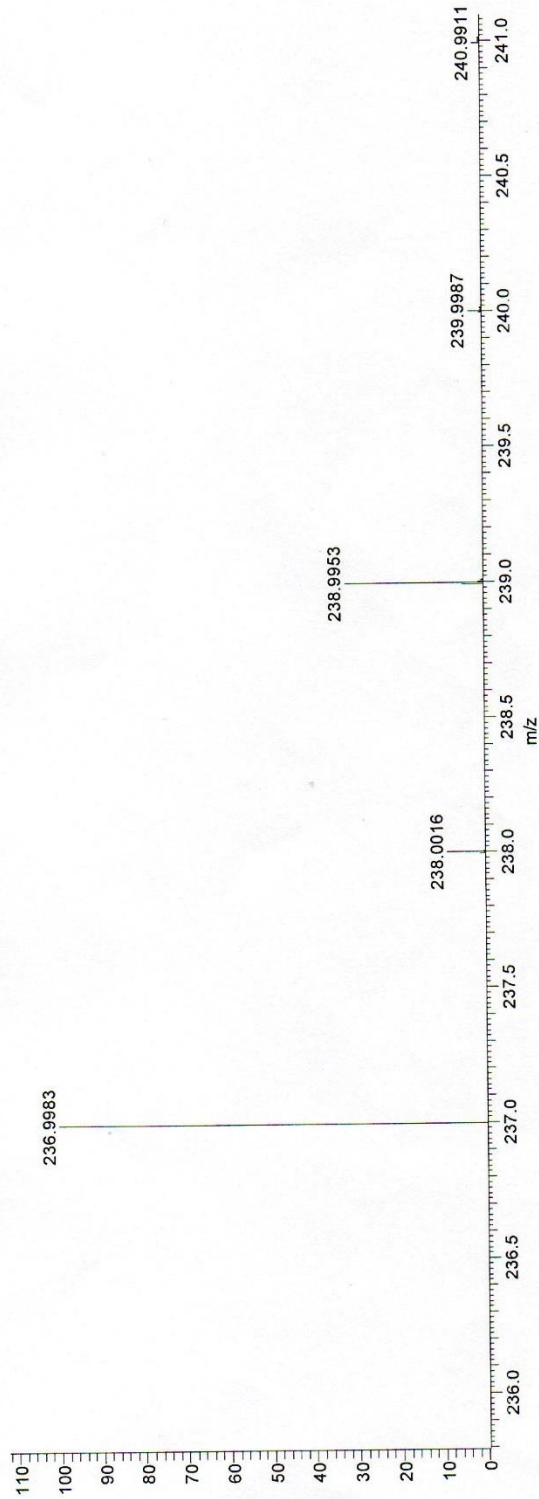


# Thermo Exactive Plus EMR Orbitrap ASAP pos

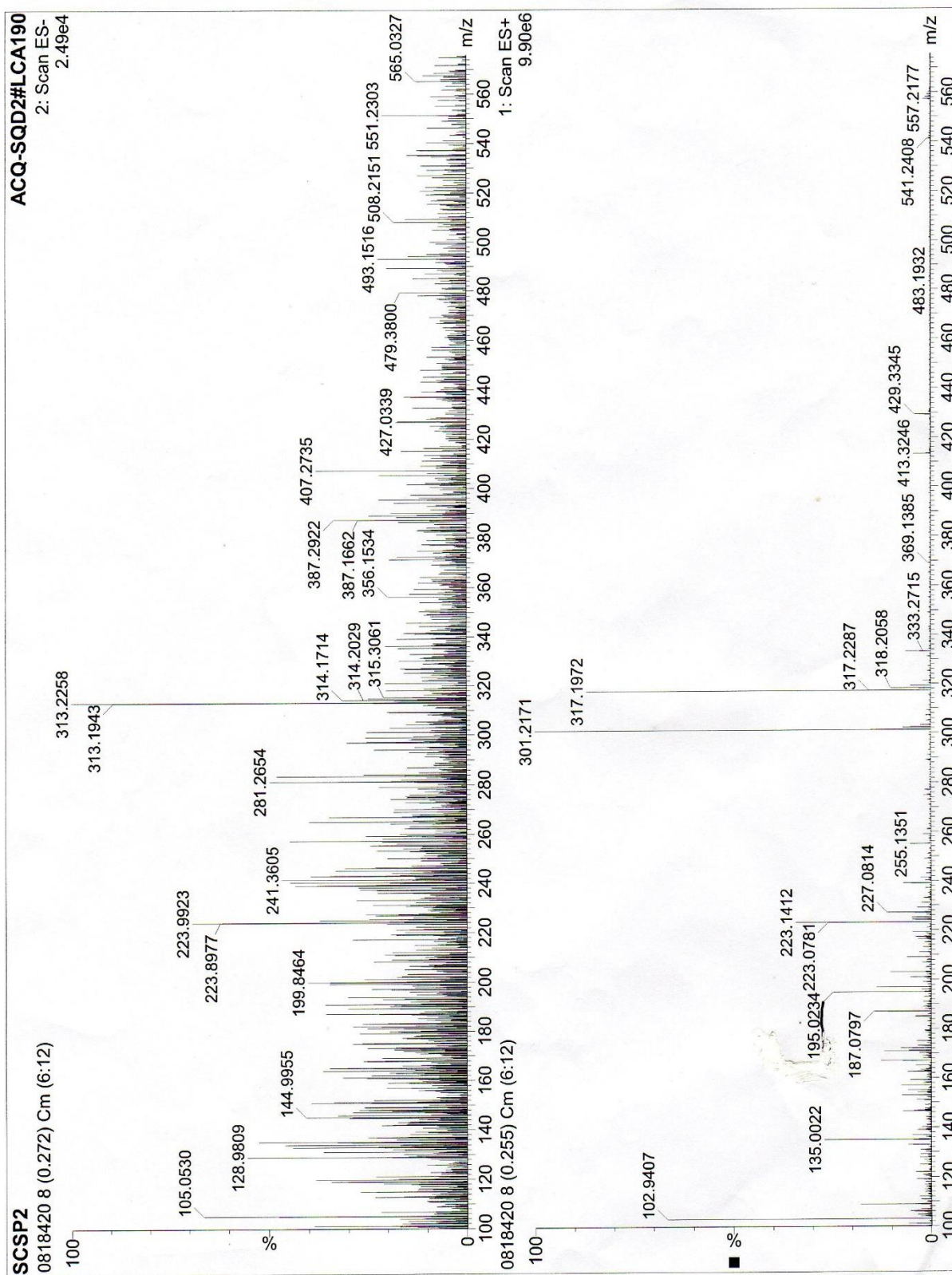
NL:  
1.64E9  
0818509ASAP#2-6  
RT: 0.09-0.27 AV: 5 T:  
FTMS + p APCI corona  
Full ms  
[100.0000-1000.0000]



NL:  
6.53E5  
C<sub>8</sub> H<sub>9</sub> ClO<sub>4</sub> SH:  
C<sub>8</sub> H<sub>10</sub> Cl<sub>1</sub> O<sub>4</sub> S<sub>1</sub>  
pa Chrg 1



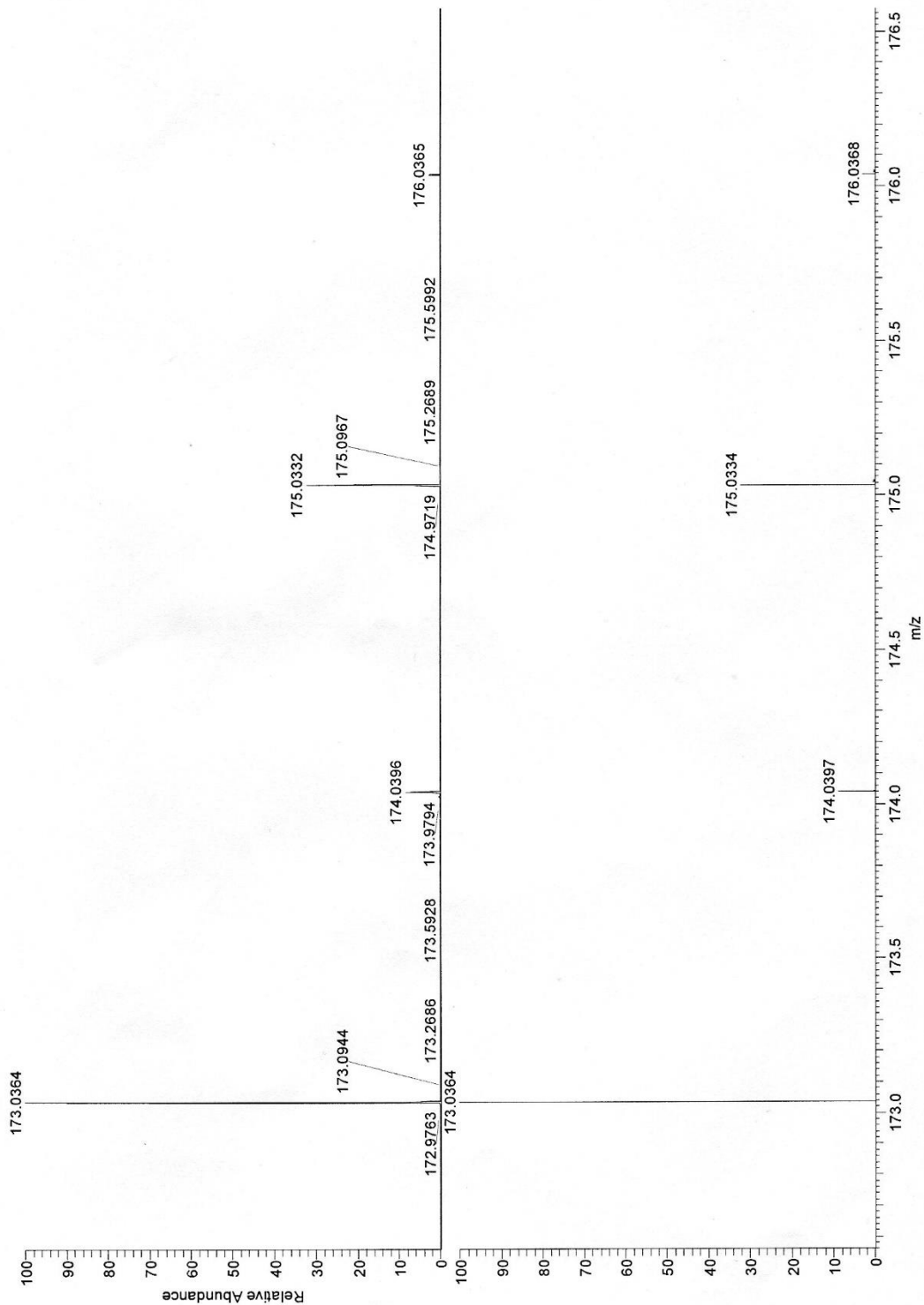
MS data for compound **60**



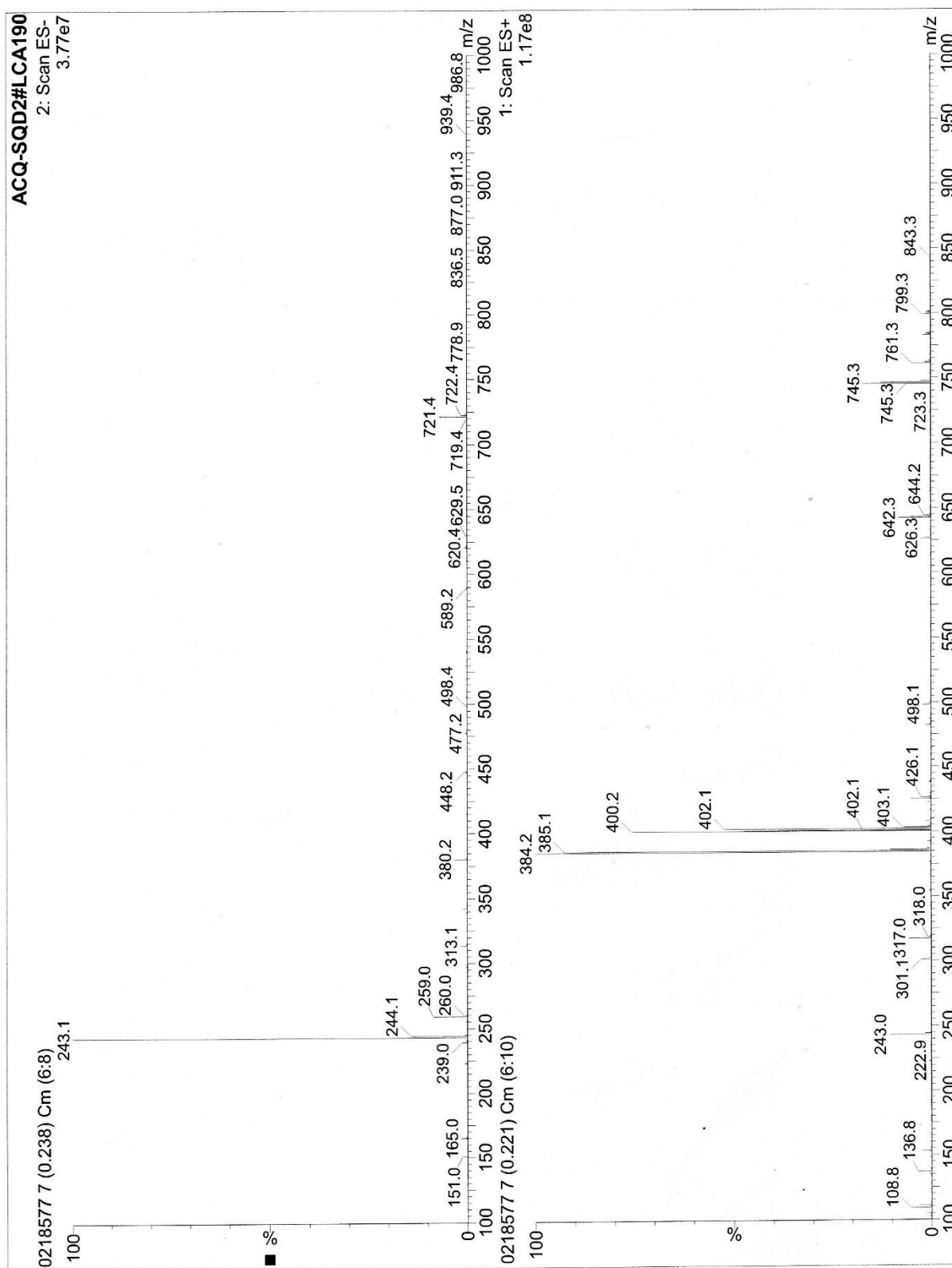
Thermo Exactive Plus EMR Orbitrap ASAP pos

NL:  
1.47E10  
0818482ASAP#1-2  
RT: 0.04-0.09 AV: 2 T:  
FTMS + p APCI corona  
Full ms  
[100.0000-1000.0000]

NL:  
6.91E5  
C8H9ClO2H  
C8H10Cl1O2  
pa Chrg 1



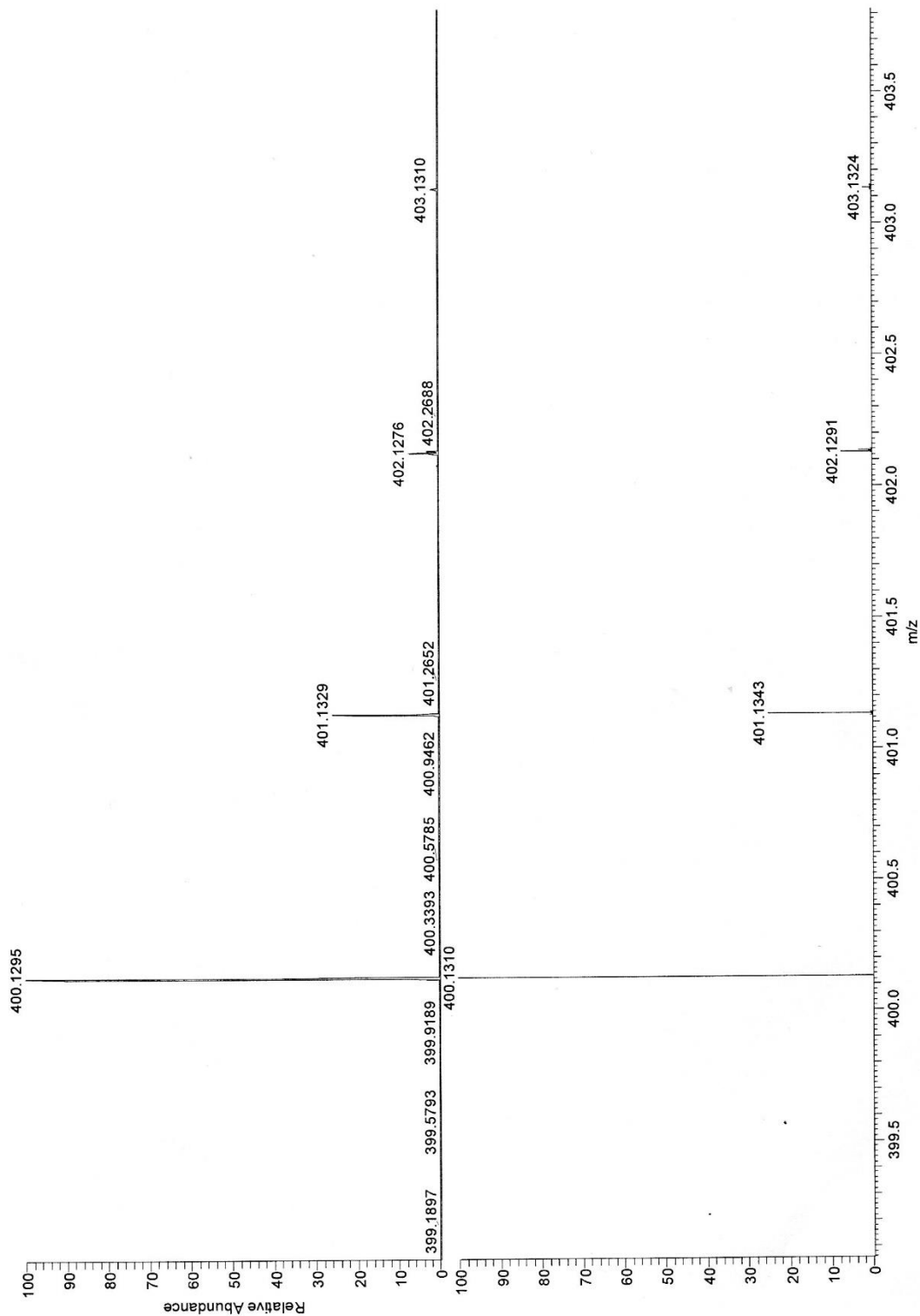
MS data for compound **7**



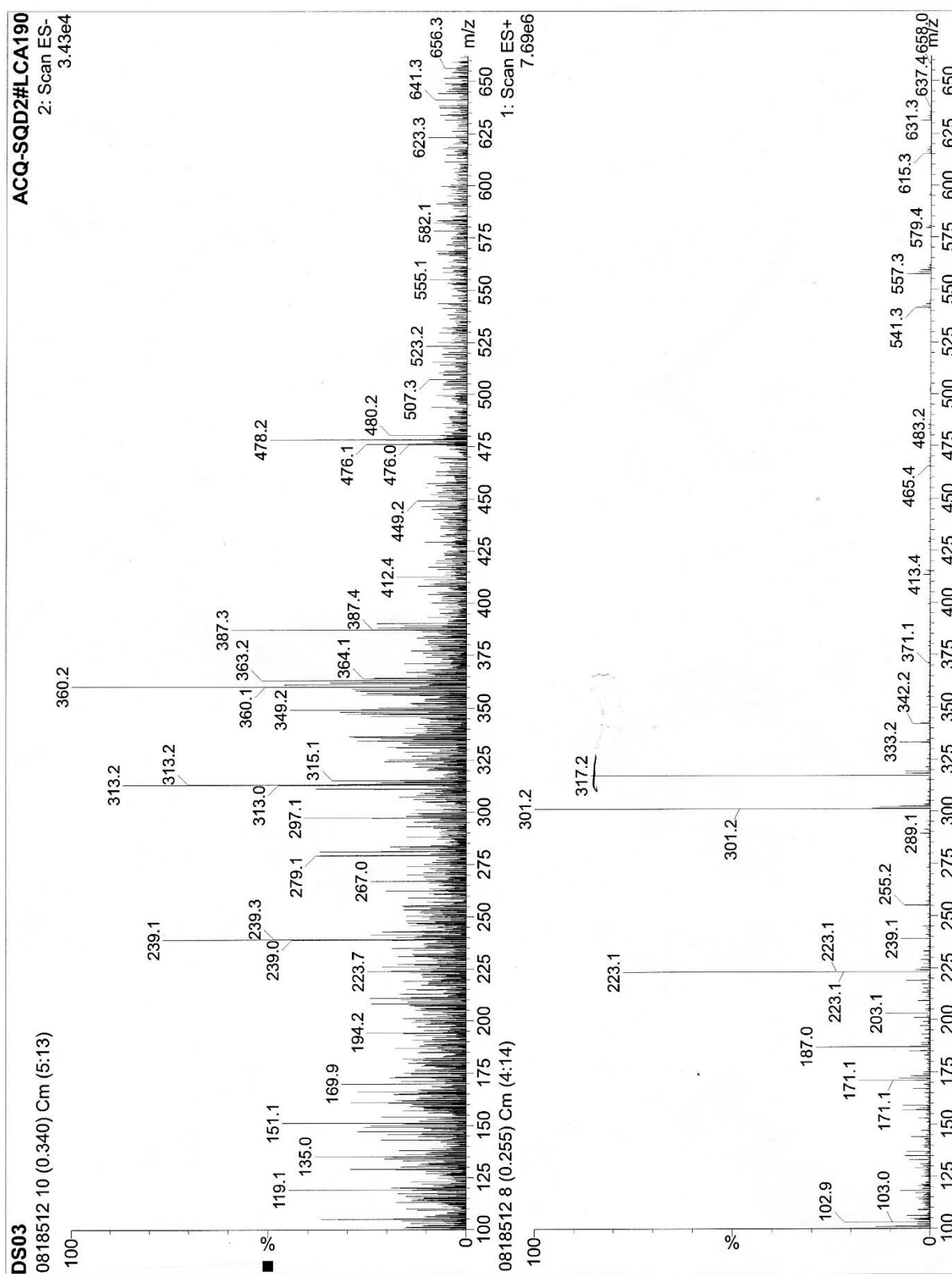
# Thermo Exactive Plus EMR Orbitrap HESI POS

NL:  
2.14E7  
03181000#9-28 RT:  
0.07-0.24 AV: 20 T:  
FTMS + p ESIFull  
ms  
[100.0000-  
1200.0000]

NL:  
7.18E5  
C<sub>23</sub> H<sub>23</sub> NO<sub>3</sub> K:  
C<sub>23</sub> H<sub>23</sub> N<sub>1</sub> O<sub>3</sub> K<sub>1</sub>  
pa Chrg 1



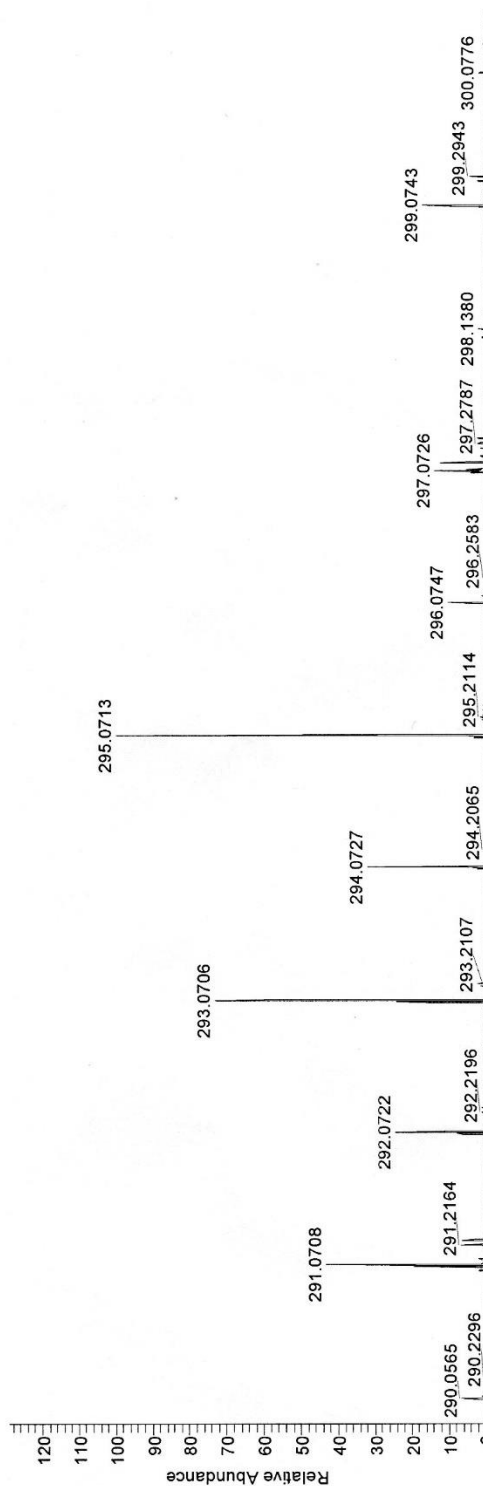
MS data for compound **54**



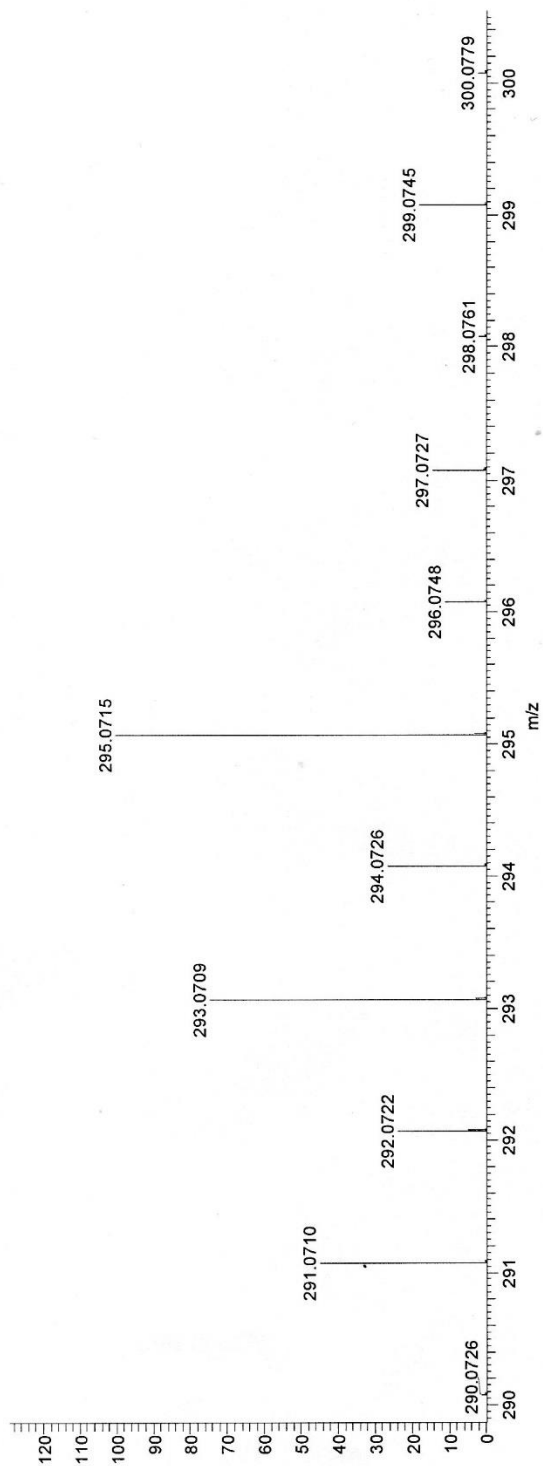


# Thermo Exactive Plus EMR Orbitrap ASAP POS

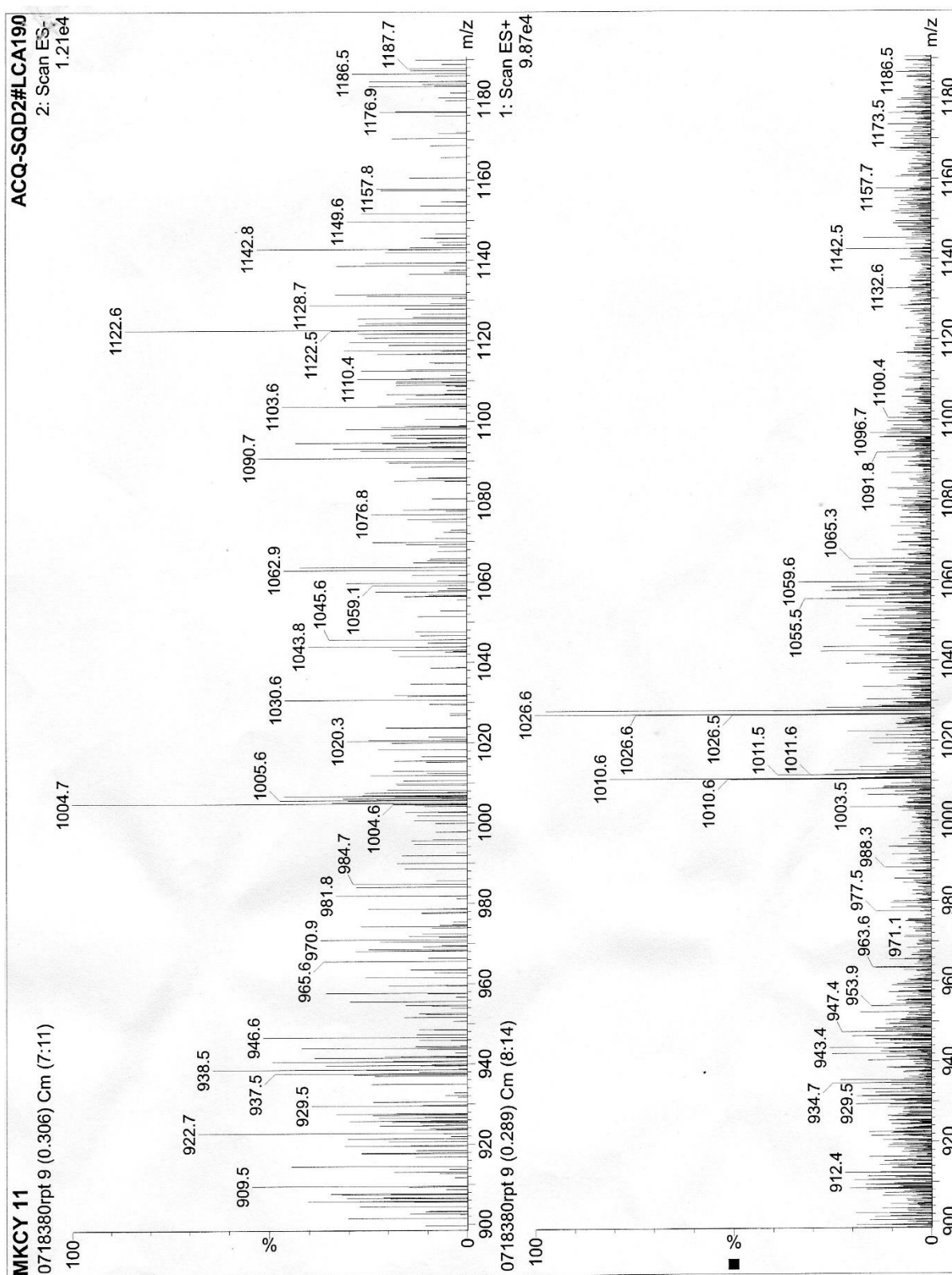
NL:  
5.12E7  
0818534ASAP-pos9-  
11 RT: 0.40-0.49 AV: 3  
T: FTMS + p APCI  
corona Full ms  
[100.0000-1000.0000]



NL:  
2.90E5  
C<sub>10</sub>H<sub>22</sub>O<sub>2</sub>SnH:  
C<sub>10</sub>H<sub>23</sub>O<sub>2</sub>Sn1  
pa Chrg 1

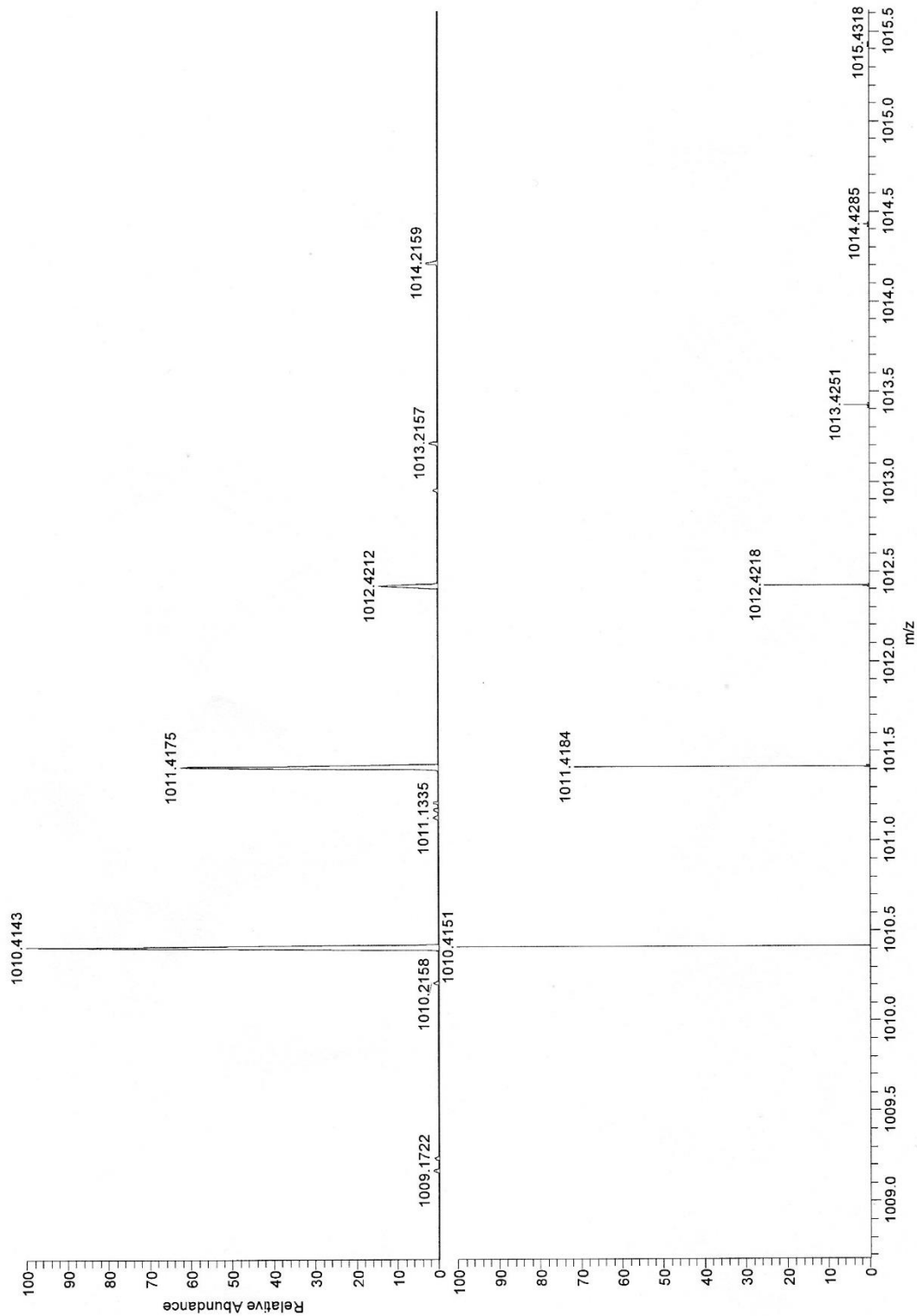


MS data for compound **8**



# Thermo Exactive Plus EMR Orbitrap HESI pos

NL:  
5.86E4  
0818508#12-24 RT:  
0.10-0.20 AV: 13 T:  
FTMS + pESI Full  
ms  
[100.0000-  
1200.0000]



NL:  
4.76E5  
C<sub>66</sub> H<sub>57</sub> N<sub>3</sub> O<sub>6</sub> Na:  
C<sub>66</sub> H<sub>57</sub> N<sub>3</sub> O<sub>6</sub> Na<sub>1</sub>  
pa Chrg -1